

Risk-Based Shelter Network Design in Flood-Prone Areas: An Application to Haiti

**Maedeh Sharbaf
Valérie Bélanger
Marilène Cherkesly
Marie-Ève Rancourt
Giovanni Michele Toglia**

March 2024

Bureau de Montréal

Université de Montréal
C.P. 6128, succ. Centre-Ville
Montréal (Québec) H3C 3J7
Tél : 1-514-343-7575
Télécopie : 1-514-343-7121

Bureau de Québec

Université Laval,
2325, rue de la Terrasse,
Pavillon Palais-Prince, local 2415
Québec (Québec) G1V 0A6
Tél : 1-418-656-2073
Télécopie : 1-418-656-2624

Risk-Based Shelter Network Design in Flood-Prone Areas: An Application to Haiti

Maedeh Sharbaf^{1,2,*}, Valérie Bélanger^{1,2}, Marilène Cherkesly^{1,3},
Marie-Ève Rancourt^{1,2}, Giovanni Michele Toglia⁴

1. Interuniversity Research Centre on Enterprise Networks, Logistics and Transportation (CIRRELT)
2. Department of Logistics and Operations Management, HEC Montréal
3. Département de management, Université du Québec à Trois-Rivières
4. World Bank, Ave. Lope de Vega No. 29, Torre Novo-Centro, Piso 10, Santo Domingo, Dominican Republic

Abstract. Evacuations occur when human safety is compromised by disasters, such as floods. Shelters play a crucial role in providing protection for individuals who have been displaced or have lost their housing, emphasizing the requirement for secure accessibility. This paper introduces a systematic optimization tool, utilizing mathematical programming, to assist decision-makers in designing effective shelter networks. We propose a risk-based approach, wherein the inherent risks of the shelter network (i.e., population, shelter, and evacuation risks) have been thoroughly assessed and measured to consider the impacts of floods based on empirical research outputs. To formulate a well-parameterized and valid problem, extensive data collection and processing, incorporating the use of geographic information systems for data management, have been conducted. In collaboration with the World Bank, this project contributes to a development initiative focused on strengthening disaster response capacity and infrastructure for Haiti, experiencing recurrent devastating floods and in need of enhancing its existing shelter network. Detailed computational results highlight the value of our risk-based methodology compared to more common approaches, emphasizing contributions to addressing real humanitarian problems.

Keywords: Shelter network design, risk assessment and optimization, location problem, floods, pedestrian-based evacuation, humanitarian logistics

Results and views expressed in this publication are the sole responsibility of the authors and do not necessarily reflect those of CIRRELT.

Les résultats et opinions contenus dans cette publication ne reflètent pas nécessairement la position du CIRRELT et n'engagent pas sa responsabilité.

* Corresponding author: maedeh.sharbaf@hec.ca

1 Introduction

The frequency of disasters has seen a significant increase over the past decades. Before 1960, there were typically fewer than 50 reported disasters worldwide per year. Since 2000, the number has consistently exceeded 335 natural disasters annually, except in 2023, when there were 239 events (EM-DAT, 2021). Floods have been the most frequently recorded disaster since 1995, with an average of 156 occurrences and a peak of 226 in 2021 (EM-DAT, 2021). Since 1980, flooding has caused more than one trillion dollars in losses worldwide, and the number of victims is estimated to double globally by 2030 (WRI, 2020). The risk of flooding is growing worldwide due to increased rainfall and storms caused by the effects of climate change, socioeconomic factors such as population growth, developments near rivers, and land subsidence caused by excessive extraction of groundwater (WRI, 2020). These trends have considerable impacts on low-income populations, particularly those in vulnerable areas with low-density road networks, where populations tend to live in informal settlements highly exposed to the effects of flood disasters (Chang and Liao, 2015). In fact, floods pose a significant threat to people's livelihoods, with approximately 23% of the world's population (1.8 billion people) exposed to this hazard, negatively affecting global development (Rentschler et al., 2022).

A crucial decision revolves around whether to initiate an evacuation when human safety is at risk, aiming to protect people from the impacts of disasters such as floods. This measure safeguards lives by relocating individuals to secure locations and providing necessary support. To ensure effective evacuations, it is imperative to establish potential shelter locations since they are vital for people who cannot evacuate to other safe places (Amideo et al., 2019). Beyond survival, shelters are a fundamental contributor to security, safety, climate protection, and resistance to diseases for disaster-prone populations (Saunders, 2013). Recognizing the importance of ensuring the protection of people affected by disasters, it is acknowledged that shelter network design problems are fundamental facility location issues related to disaster operations management (Ozbay et al., 2019). Shelter network design problems often represent decisions made in the preparedness phase of disaster management as part of evacuation planning, which in turn depend on the characteristics of the modeled systems. Anticipating the state of the network post-disaster and its contingent risks is challenging but must be considered to efficiently determine shelter locations.

The Sphere Handbook (Sphere Association, 2018), which sets post-disaster sheltering standards, emphasizes that service points should be established where they are safe and most convenient for the beneficiaries, not solely based on logistic convenience for the providing agency. Damages to infrastructure and people's vulnerability can also negatively affect accessibility and hamper evacuation to shelters. Therefore, when developing methodologies to design and optimize shelter networks, considering both network features and the people who will evacuate is essential. Moreover, embedding response considerations (e.g., risk encountered in reaching a shelter in a flooded area) in preparedness decisions (e.g., shelter locations) leads to more effective disaster management (Van Wassenhove, 2006). To address the lack of realistic assumptions in shelter location and evacuation planning, problems should be more application-oriented rather than theoretical or model-driven, as noted by (Amideo et al., 2019). Understanding the context, evaluating the key considerations and particularities, and defining constraints and objectives of the stakeholders are crucial aspects of such problem formulation.

While ensuring that shelters are located in safe places to cover the most vulnerable population, it is

also essential to understand how people evacuate from their households to shelters and the level of risk they face on their path when planning for and modeling effective evacuation (Lim et al., 2016). Pedestrian-based evacuations, where people walk to secure zones or shelters, are common due to limited access to personal vehicles, a lack of public evacuation transport, road congestion, and damages (Lim et al., 2016; Wood et al., 2018). This is especially prevalent in developing countries, although it also occurs in developed countries. For instance, Bangladesh, which faces threats from severe storms exacerbated by climate change, continually experiences devastating floods (with an average of 21% of the country being flooded every year), and people often have to evacuate by walking through water to reach shelters. Similar events also occur in the Philippines, Haiti, Japan, and other countries.

The aim of this paper is to introduce a systematic optimization tool, utilizing mathematical programming, to assist decision-makers in designing effective shelter networks. We propose a risk-based approach, thoroughly assessing and measuring the inherent risks of the shelter network (population, shelter, and evacuation risks). This assessment considers vulnerability and the impacts of floods, with risks measured based on previous empirical research outputs. To ensure relevance, validity, and practical applicability throughout the development of this decision support tool, we collaborated with the World Bank as part of an initiative focused on strengthening disaster response capacity and improving infrastructure in Haiti – specifically, the Haiti- Strengthening Disaster Risk Management and Climate Resilience Project (H-SDRMCRP) (World Bank, 2019a). We now describe in more detail the problem and contributions of this study.

1.1 Problem description and context of this study

Several developing countries, like Haiti, struggle with insufficient capacities and inadequate local shelter networks. While communities often turn to public infrastructures such as schools, churches, and municipal halls for sheltering needs, these facilities may lack the necessary conditions, such as proper sanitation and cooking facilities, to offer suitable shelter for an extended duration. As these facilities, intended for short-term shelter, are often used for longer periods, additional challenges arise. Moreover, they may not adequately cover those facing the most risk or vulnerability, and people may encounter significant risks when trying to reach them, especially when they have to walk long distances through water.

The Risk-Based Shelter Location Problem (RB-SLP) addressed in this paper involves deciding where to construct new shelters (i.e., shelter-location decisions) with the aim of maximizing the population enfold risk and minimizing the shelter and network risk under coverage, budget, and capacity constraints. It also involves determining to which shelter the covered population should evacuate to (i.e., population-shelter assignment decisions). More precisely, the three main components of the objective include: 1) maximizing the population risk covered by the shelter network, 2) minimizing the risk associated with new shelter locations, and 3) minimizing the evacuation risk encountered by the population when they reach their assigned shelter. Overall, population and shelter risk factors include exposure to flood hazards, the potential sheltering coverage provided by existing infrastructure, and vulnerability (measured by a series of indices accounting for wealth and the quality of infrastructure). Concurrently, evacuation risk considers the challenges associated with walking through water. Further details on the measurement of each risk are provided in Sections 4 and 5.

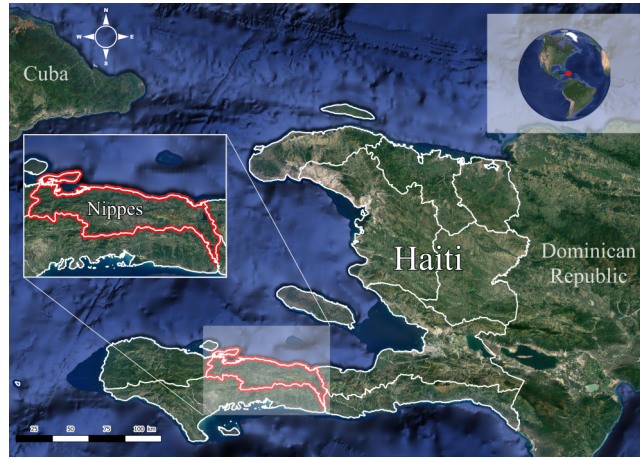


Fig. 1: Map of the Nippes Department of Haiti

The RB-SLP is formulated on a graph with population points and potential locations for new shelters. Each population point is associated with an estimated number of people in need of sheltering services (i.e., the demand), determined by the population and a percentage of sheltering need. Potential new shelter locations must meet specific criteria, including low flood risk and road accessibility. Shelters, in accordance with humanitarian or national standards, should cover a population within a designated radius to limit walking distances and adhere to capacity limits based on the maximum required square footage per person. The construction of new shelters incurs costs, including building expenses and others dependent on factors like ownership, terrain type, and infrastructure availability (e.g., electricity, water, sanitation, landscaping). Decisions are made under budget constraints and predetermined financing limits for shelter network improvement. In this paper, we assume the entire investment is allocated to new constructions, but in practice, planners might leverage parts of the existing infrastructure that remain functional and enhance them. Although our methodology is developed to solve the RB-SLP focusing on new constructions, it can easily adapt to cases involving partial network reconstruction and improvement. The proposed solution aims to support governmental entities and other decision makers involved in supporting local authorities to optimize the value provided by their investments and design efficient shelter network and evacuation plans.

For this study, we parameterized and tested RB-SLP to enhance the shelter network in the Nippes Department of Haiti (Figure 1). Haiti, ranking third among countries most affected by weather-related disasters (Eckstein et al., 2019), is one of the world’s poorest nations (World Bank, 2022). The country faces multiple hazards, with over 96% of the population exposed to two or more, including floods, hurricanes, earthquakes, and landslides (Llopis Abella et al., 2020). The severe human and economic impact of disasters is exacerbated by Haiti’s hazard exposure and infrastructure vulnerability (Llopis Abella et al., 2020). Despite some progress, Haiti still lacks adequate preparedness and resilience-building mechanisms, especially considering the expected increase in the frequency, intensity, and impacts of extreme weather events due to climate change (World Bank, 2022). After a flood, the affected population finds temporary housing in shelters. Existing buildings, such as schools, auditoriums, churches, and other public structures, can serve as shelters (referred to as existing shelters). However, using these buildings for an extended period poses challenges. Firstly, it disrupts their primary activities, and secondly, they often lack essential amenities and may not comply with building codes, making them unsafe due to potential safety or flooding issues – many are situated in high flood-prone areas.

Haiti faces insufficient shelter capacity, necessitating the expansion and enhancement of its network ([World Bank, 2019a](#)). Given the high flood hazard in the Nippes Department of Haiti, it serves as a crucial case for testing and validating our methodological approach. Throughout the development of our risk-based approach, our aim has been to support the government of Haiti and the World Bank, which is committed to addressing the sheltering issue through their financed project, H-SDRMCRP.

1.2 Challenges, contributions, and organization of this paper

In this section, we synthesize the contributions and related challenges of this study, as well as present the general organization of this paper. The contribution of our study is threefold: firstly, proposing a new optimization model; secondly, innovating data gathering and processing methods; and thirdly, conducting thorough analysis and facilitating the transfer of knowledge and recommendations to practitioners.

To the best of our knowledge, our proposed methodology is the first attempt toward shelter network optimization in the context of pedestrian-based evacuation in flood-prone areas, where risk accounting for hazard, exposure, and vulnerability is considered for all the network components: shelters (i.e., supply), populations (i.e., demand), and the evacuation paths (i.e., network edges). We proposed a novel and practical optimization model that takes into account several significant factors driving needs and risks (e.g., flood hazards, population density, vulnerability, current shelter capacities, road accessibility, etc.) to offer efficient holistic solutions for designing or strengthening shelter networks. We also propose innovative approaches to model flood-related risk for each network component by integrating the outputs of data science methods from various disciplines, including hydrology, socio-demographic analysis, Geographic Information Science (GIScience), and mathematical programming. As opposed to studies that proposed optimization models for disaster preparedness in general cases ([Sabbaghtorkan et al., 2020](#)), we specifically focus on floods, which are frequent and have high impacts every year. This allows to fully grasp their characteristics and incorporate the driving factors of their impacts on shelter networks into our decision support tool.

It is recognized that data collection and accessibility pose significant challenges in the humanitarian sector, lacking formal digital processes and often involving scattered data across multiple stakeholders ([Besiou et al., 2018](#); [Gupta et al., 2019](#); [Kovacs et al., 2019](#); [Kunz et al., 2017](#); [Lukosch and Comes, 2019](#); [Pedraza-Martinez et al., 2013](#); [Van Wassenhove, 2006](#)). Difficulties also arise in understanding contexts and defining problems in developing countries ([Rancourt et al., 2015](#)). Collaborative studies with field practitioners in humanitarian operations management are crucial to overcoming these issues ([Pedraza-Martinez and Van Wassenhove, 2016](#)). For this project, our collaboration with the World Bank and the Government of Haiti allowed the formulation of a well-defined and realistic problem, adequately parameterized using unstructured information from discussions with partners and data extracted from formal tools such as Geographical Information System (GIS). In order to measure risk in a disaggregated and small geographical scale – from almost household level to precise potential shelter locations like public schools – extensive data processing and analysis were required. We processed and integrated various geospatial data sources, including information extracted from high-resolution flood hazard maps, OpenStreetMap, vulnerability indices, demographic data, etc., mostly using a GIS to construct and parameterize the underlying network in our region of interest, specifically the Nippes

Department of Haiti. This approach enabled us to consider several pertinent factors related to hazard, exposure, and vulnerability, thus facilitating risk estimation for the network. These estimations were further refined by incorporating contextual knowledge from our partners and findings from empirical studies, such as those examining the influence of water depth on human walking speed (Bernardini et al., 2020). This process resulted in the development of a novel and practical model for shelter network design, which underwent comprehensive testing and validation.

While our methodological contribution is generally applicable and replicable for countries addressing flood-related challenges and aiming to enhance their sheltering capacity, we consider our collaboration as an essential component of this research project, grounded in a real-life application. Extensive computational analyses were conducted to ensure robustness and correctness, while demonstrating the efficacy of our risk-based methodology compared to more conventional approaches. Sensitivity analyses were also performed to assess the impact of costs and budget constraints on network effectiveness. These allowed to perform analyses and consider several factors and scenarios which were not possible by means of more traditional approaches implemented by our partners. The solution approach was validated by the H-SDRMCRP technical team, and our method have been extended to make recommendations on possible shelter locations in another department of Haiti, namely Nord-Ouest Department, which have been used for further field investigation by the Government. This highlights our scientific and practical contributions in addressing a crucial decision-making and design problem within the humanitarian and public safety sectors, leveraging data-science methodologies. We bridge the gap between practice and academia for shelter network design and evacuation planning in developing countries, offering implementable solutions within a real-life setting.

The remainder of this paper is organized as follows. Section 2 reviews the relevant literature. In Section 3, we introduce the proposed risk-based model along with the associated mathematical notation. Section 4 outlines our risk assessment methodology, providing an overview of how risk is defined in the literature and detailing the adaptation of each risk element to the three proposed risk measures. In Section 5, we present the specific case of Haiti, detailing the data collection, processing, and analysis procedures. Detailed computational results are reported in Section 6 to assess the performance of our risk-based approach compared with standard approaches, including a comparison with our partners' solution. We further conduct sensitivity analyses on key parameters. Conclusions are then provided in Section 7.

2 Literature review

Responding to a disaster requires the management of complex supply chains, which is essential to meet the objectives of humanitarian aid. In particular, humanitarian logistics can play a crucial role in the mitigation, preparation, response, and recovery of sudden-onset disasters (Behl and Dutta, 2019; Besiou and Van Wassenhove, 2020; Çelik et al., 2012; De Vries and Van Wassenhove, 2020; Kara and Savaşer, 2017; Kovacs and Moshtari, 2019). While there has been growth in humanitarian relief literature, the majority of the studies are of qualitative nature, leaving a gap in quantitative research methods (Chiappetta Jabbour et al., 2019). The recent surge in natural disasters has, however, increased interest in quantitative methods for humanitarian logistics. To this aim, operations research methodologies can make significant contributions to adapt supply chain practices to humanitarian logistics (Altay and Green III, 2006; Laporte, 2023), especially in developing countries (White et al.,

2011).

Evacuation is one of the most important steps during the response phase, serving as the primary strategy to protect people from potential disaster impacts (Bayram, 2016). Location problems are often solved during the mitigation and preparedness phases (Paul and Wang, 2019; Arslan et al., 2021), while evacuation operations happen during the response phase (Amideo et al., 2019). Influenced by factors such as nature of the disaster (e.g., flood, hurricane, earthquake) and transportation mode (e.g., foot, car, bus, train, boat, and helicopter), three types of evacuation can occur: (i) self-evacuation, which includes evacuees who move towards shelters autonomously without any assistance from emergency services; (ii) assisted evacuation, which involves individuals who can arrange their own evacuation towards shelters but need some advice and guidance (e.g., directions) from authorities; and (iii) supported evacuation, which might be designed for special-needs populations (e.g., elderly, disabled) who require support from public authorities to reach designated shelter facilities (Amideo et al., 2019). In the event of an evacuation, shelters are fundamental contributors to security and safety, climate protection, and resistance to diseases for affected communities (Amideo et al., 2019). Poorly located shelters can increase the risks faced by individuals and enhance exposure to hazards (Saunders, 2013). Shelter site location and evacuation planning, i.e., the process of relocating individuals from their residences to predetermined safety zones, are therefore pivotal components of effective disaster response. Nonetheless, the majority of research has tended to analyze these two related problems separately, potentially leading to inefficient solutions (Amideo et al., 2019). Few studies have considered the interdependencies between shelter location and evacuation planning, considering how each influences the other.

This section examines the literature pertinent to shelter site location. We first review two distinct categories of research: (i) studies under deterministic setting, where all data is assumed to be known in advance; (ii) studies under stochastic setting, where the data is subjected to different sources of uncertainty. Then, we discuss studies that specifically focused on flood disasters, including the ones related to evacuation planning. Finally, we position our contributions within the existing literature. We refer the reader to Farahani et al. (2020) and Sabbaghtorkan et al. (2020) for comprehensive reviews on location decisions in humanitarian supply chains.

2.1 Deterministic shelter location studies

Deterministic studies assume that all parameters of the underlying problem, e.g., the number of individuals in need of shelter, are known with certainty. In this setting, many authors relied on a multi-objective approach to capture the various dimensions of shelter location problem. Following this approach, Alçada-Almeida et al. (2009) developed a multi-objective model to locate temporary shelters and identify primary evacuation routes in the context of wildfire. The model aims to minimize travel distance and fire risk associated with travelling on evacuation paths or staying in shelters using a predetermined “Fire Risk Index Method.” Coutinho-Rodrigues et al. (2012) extended the work of Alçada-Almeida et al. (2009) by adding objectives to minimize the number of open shelters and travel distance on a secondary evacuation path, which is used if the primary path is impassable. Doerner et al. (2009) also relied on a multi-objective model to locate shelters in the southern Sri Lanka, a tsunami-prone area, considering public facilities (e.g., schools) as candidate locations. The objectives include maximizing coverage, minimizing cost, and minimizing risk of inundation at new

shelters based on the probability of future tsunami occurrence. To find optimal location for temporary shelters during a flood disaster, [Chanta and Sangsawang \(2012\)](#) developed a bi-objective model to maximize the coverage and minimize the weighted travel distance. [Kilci et al. \(2015\)](#) proposed a model to determine the location of temporary shelter sites, assign population points to the closest shelters, and control utilization rate of open shelters with the goal of improving the Turkish Red Crescent operations. Each candidate shelter location was scored with respect to ten different criteria (e.g., transportation of relief items, road connections, healthcare providers), with the objective to maximize the minimum score of open shelters. Finally, [Hallak et al. \(2019\)](#) developed a multi-objective model to optimize shelter locations and assignments. The objectives balance multiple factors, including covering basic and special needs, future expandability of shelters, employment opportunities at shelters, and cost-efficiency.

While the location of shelters is critical, additional facilities such as medical centers may be needed to meet evacuees' needs and contribute to relief effort. Some authors have therefore developed models that extend beyond shelter locations to incorporate more explicitly various components of disaster response. Following this approach, [Sheu and Pan \(2014\)](#) proposed a centralized emergency supply network to identify not only the locations of shelters, but also the location of medical and distribution centers. The model minimizes operational costs and travel distance as well as psychological costs experienced by affected individuals. Similarly, [Rodríguez-Espíndola and Gaytán \(2015\)](#) developed a bi-objective optimization model to determine the locations of shelters and distribution centers that minimize cost and travel distance. Finally, a comprehensive multi-objective model to guide decision-making in disaster preparedness was elaborated by [Rodríguez-Espíndola et al. \(2018\)](#). This model still identifies facility locations (i.e., shelters and distribution centers), but also include stock prepositioning, resource allocation, and relief distribution with the aim of minimizing the total cost.

Disasters are inherently time-dependent, with their impact and required response evolving over time. This dynamic nature underscores the necessity to capture the temporal aspects of disasters in the modeling process, ensuring solutions are both effective and adaptable to changing conditions. Some studies explore this avenue and incorporate time-dependent aspects into shelter location problem. This is the case of the multi-period optimization model proposed by [Gama et al. \(2016\)](#). The latter seeks to determine the opening times and locations of shelters, timings for evacuation order dissemination, and shelter assignment while minimizing the total travel time. [Chen et al. \(2013\)](#) introduced a three-level hierarchical shelter location model that accounts for evacuee's evolving needs over time, considering three types of shelters to serve immediate, short-term, and long-term needs. [Pérez-Galarce et al. \(2017\)](#) also rely on a hierarchical shelter location model to optimize shelter locations. In their study, two types of shelters with successively inclusive levels are considered, namely basic service shelters and medical/psychological service shelters. The model aims to minimize travel distance while considering shelter capacities and utilization rates.

2.2 Stochastic shelter location studies

Reviews highlight the importance of capturing uncertainty in disaster operations ([Dönmez et al., 2021](#); [Hoyos et al., 2015](#); [Liberatore et al., 2013](#)). In shelter location problem, dealing with uncertainty is difficult due to the chaotic circumstances associated with the post-disaster phase as well as multiple stakeholder structure. While different paradigms (e.g., stochastic programming, chance-

constrained programming) have been used in the literature to capture the uncertainty in shelter location problem, stochastic programming has emerged as the most popular modeling framework. [Li et al. \(2011\)](#) introduced a two-stage stochastic programming model that accounts for uncertain demand and transportation cost. The model aims to determine shelter locations and their capacities, while also allocating evacuees and commodities to these shelters, with the ultimate objective of minimizing the total cost. [Li et al. \(2012\)](#) rather proposed a scenario-based bi-level programming model to analyze how shelter location decisions affect drivers' route choices in possible hurricane scenarios. This model considers uncertainties in demand, shelter disruptions, and road accessibility. In the upper-level, a two-stage stochastic process identifies shelter locations pre-disaster and decides on shelter openings and evacuee allocations post-disaster. The lower-level models drivers' route choices using a user equilibrium approach. [Bayram and Yaman \(2018\)](#) proposed a two-stage stochastic model that accounts for uncertainty in evacuation demand, road network conditions, and disruption in shelters. The model aims to identify location of shelters and allocation of evacuees to shelters and routes while minimizing the expected total evacuation time. [Ozbay et al. \(2019\)](#) considered secondary disaster following the main disaster and proposed a three-stage stochastic programming model with uncertainty in demand. Temporary shelters for the main and secondary disasters are located in the first and second stages, and affected population are allocated to the nearest shelters, in the second and third stages. The objective is to minimize the expected number of open shelters while maximizing their weights. A chance-constrained model was introduced by [Kinay et al. \(2018\)](#) by considering uncertainty in demand with two types of probabilistic constraints: one concerning the utilization rate of shelters and the other concerning their capacity. The authors considered the deterministic model proposed by [Kilci et al. \(2015\)](#) as starting point and proposed a probabilistic programming model to maximize the minimum score of open shelters. [Kinay et al. \(2019\)](#) extends the work of [Kinay et al. \(2018\)](#) following a multi-criteria framework. In addition to the original objective, two more objectives are added: maximizing the average score of selected shelters and minimizing the average distance traveled by evacuees. [Dalal and Üster \(2018\)](#) developed a combined stochastic-robust optimization model to optimize the location of shelters and distribution centers as well as assignments and flows. The model aims to minimize the weighted sum of average and worst-case transportation costs across all scenarios while considering demand uncertainty. The model can function as either a two-stage stochastic program, a robust optimization approach, or a mixed robust-stochastic setting, depending on the objective considered. Finally, [Song et al. \(2019\)](#) proposed a multi-criteria decision-making method to rank potential shelter locations considering environmental conservation, transportation accessibility, and social sustainability. They employed interval rough number transformation to address uncertainty, subjectivity, and ambiguity in the shelter-site evaluation process.

2.3 Specific applications to flood disaster

Different disasters necessitate different evacuation plans and may utilize diverse transportation modes. Previous studies, such as [Haynes et al. \(2009\)](#), cautioned against generalizing evacuation strategies across different types of natural hazards. [Baker \(1991\)](#) also warned researchers against extrapolating findings from one hazard to another. Therefore, a hazard-specific approach to evacuation is necessary, as strategies effective for one type of hazard may not be safe or suitable for others ([Scanlon, 1992](#)). To our knowledge, few studies have developed evacuation plans and shelter location models specifically for flood-prone areas, as we have in our work. In fact, only [Chanta and Sangsawang \(2012\)](#), [Rodríguez-Espíndola and Gaytán \(2015\)](#), [Rodríguez-Espíndola et al. \(2018\)](#), and [Gama et al. \(2016\)](#)

have proposed shelter location models in the specific context of floods (see Section 2.1 for details). However, these studies tend to overlook some important concerns related to flood evacuations, such as the mode of transportation, limited access to certain areas, and safety concerns. Under flood circumstances, evacuation may be carried out using a combination of land (e.g., walking (Eom et al., 2022), personal vehicle (Kongsomsaksakul et al., 2005), bus (Insani et al., 2022)), water (e.g., boat), and air (e.g., helicopter (Khalilpourazari and Pasandideh, 2021)) transportation.

In developed countries, where most research has been conducted, individuals typically evacuate using personal vehicles or public transportation. Consequently, a substantial portion of the literature concentrates on large-scale emergency evacuation planning, without specific shelter location considerations (Bayram, 2016). In developing countries, which warrant further research, due to the limited access to personal vehicles and the lack of public transportation systems often leave walking as the only viable option (Lim et al., 2016). Even in developed countries, pedestrian evacuation becomes increasingly important when roads are congested or rendered impassable by disasters (Wood et al., 2018). For additional examples of pedestrian evacuation in disaster contexts, refer to (Barnes et al., 2021; Bernardini et al., 2021; Eom et al., 2022; Ercolano, 2008; Faucher et al., 2020; Jin et al., 2021; Nakanishi et al., 2019; Wood et al., 2016, 2018). Therefore, recognizing pedestrian evacuation as an essential response mechanism in flood scenarios is crucial, as it could yield solutions that are not only specific to flood conditions but also sensitive to the reality of vulnerable populations.

2.4 Positioning of our study among the related literature

This paper aims to tackle the shelter location problem and evacuation planning in flood-prone regions. As opposed to many studies in the literature that focus on locating temporary shelters, e.g. tents or mobile units at the tactical decision level, we seek to strategically locate permanent relief shelter infrastructures, i.e., dispensing points where individuals receive various forms of service and humanitarian aid (Kara and Rancourt, 2019), as a means of providing protection, safety, security, and privacy to people who have left or lost their housing as a result of a disaster. Indeed, after a disaster, shelters may be needed for several months or even years until displaced people can be housed in their restored dwellings or new homes. In addition, through our literature review, we observe that disaster-specific optimization tool on shelter location and evacuation planning is rather limited. Most papers in OR/MS literature of shelter location problem consider preparation for “general” type of disasters, and primarily rely on data from developed countries. This has motivated us to investigate the shelter location and evacuation planning problem within a developing country through the use of a mathematical programming based methodology and by collaborating with the World Bank to gather contextual information and data, an approach not commonly used (Amideo et al., 2019; De Vries and Van Wassenhove, 2020) although its relevance.

Another distinctive aspect of our study lies in the unique integration of shelter location and evacuation operations, setting it apart from the existing body of literature. Combined shelter location and evacuation planning problems have typically focused on evacuation using private vehicles (i.e., car-based) or mass-transit systems (i.e., bus-based), as noted by Amideo et al. (2019). We aim to contribute to this area of literature by proposing a model focusing on “shelter location and pedestrian-based evacuation”. We focus on flood-prone areas in developing countries to fully grasp the characteristics of pedestrian evacuation and effectively incorporate their impacts in our decision support tool. Our

study uniquely integrates the impact of bodies of water on walking speed, an important consideration often overlooked in existing models.

The most distinct part of our study is how we process data to conceptualize and address uncertainty in shelter location problem. Papers in this streams of literature mostly rely on scenario-based stochastic models. However, the scarcity of past disasters and limited historical data can lead to inaccurate predictions if too much reliance is placed on using this historical information (Arnette and Zobel, 2019). Galindo and Batta (2013) stated two main drawbacks of scenario-based approach: (i) scenarios do not cover all the possible outcomes, and (ii) the set of scenarios is often considered as given input, without an efficient, systematic, and reliable method to define them. The authors argued that a more appropriate approach would involve conducting a thorough probabilistic analysis of the potential outcomes of a disaster. Risk-based approach is a deterministic alternative to scenario-based stochastic models when uncertainty is difficult to model due to lack of disaster-related data (Dönmez et al., 2021).

Only few studies proposed risk-based approach in disaster preparedness and response. Akgün et al. (2015) examined the risk associated with a demand point and applied fault tree analysis to compute the vulnerability of a demand point (i.e., the probability that it is not supported by the facilities). The risk of a demand point is calculated by the multiplication of probability of threat, vulnerability of demand point, and consequences at the demand point (value or possible loss at the demand point due to threat). A risk-based approach was also proposed by Arnette and Zobel (2019) for prepositioning relief items in the pre-disaster phase. The treatment of risk in Arnette and Zobel (2019) is similar to the work of Akgün et al. (2015). It encompasses three different components (i.e., product of hazard, exposure, and vulnerability) and focuses on the risk to the population. Although the risk-based method has been investigated, there are still research spaces for new attempts to extend this method in a facility location decision environment. Based on a review by Boonmee et al. (2017), risk is among the major criteria in emergency humanitarian logistics problems and new objectives focused on risk should be developed. To the best of our knowledge, there is no study that uses risk measures to cope with uncertainty in a shelter location problem as we do. Similar to the work of Akgün et al. (2015) and Arnette and Zobel (2019), in our approach, risk will be reflected through the product of hazard, exposure, and vulnerability. However, we develop risk measures not only for the demand, but also for the supply and edges of the network, processing socioeconomic and geological data using GIS.

3 Mathematical formulation

The RB-SLP is defined on an undirected graph $G = (V, E)$, where V is the set of vertices and E the set of edges. $V = I \cup J \cup J'$ comprises the set of population points I , the set of potential shelter locations J , and the set of existing shelters J' . Each population point $i \in I$ is associated with a population in need of shelter p_i and a normalized population risk \tilde{r}_i^p . Each shelter $j \in J \cup J'$ is associated with a capacity q_j representing the maximal number of people that can be assigned to that shelter, and with its normalized shelter risk \tilde{r}_j^s . In addition, each potential shelter $j \in J$ has a cost $c_j \geq 0$, representing the cost of locating (building) a shelter in location j . Each edge $(i, j) \in E, i \in I, j \in J \cup J'$ is associated with its travel distance d_{ij} and its normalized evacuation risk \tilde{r}_{ij}^e . Each shelter can cover population points within a maximal coverage radius r . Therefore, we define $W_j(r) \subseteq I$ as the set of population points located within a coverage radius r from shelter location j , i.e., $W_j(r) = \{i \in I | d_{ij} \leq r\}, j \in J \cup J'$. We also define $V_i(r) \subseteq J \cup J'$ as the set of shelters located within a coverage radius of r from popula-

tion point i , i.e., $V_i(r) = \{j \in J \cup J' \mid d_{ij} \leq r\}$. The maximal budget to locate (build) new shelters is B .

In the RB-SLP, the decisions consist of opening new shelters and determining which population points to assign to each of these new shelters. Therefore, we define two sets of decision variables. First, y_j is a binary variable equal to one if and only if a new shelter is located (built) at vertex $j \in J$, and zero otherwise. Second, x_{ij} is a continuous variable representing the proportion of population from $i \in I$ assigned to shelter $j \in J$. The RB-SLP can be formulated as follows:

$$\begin{aligned}
\text{Model 1} \quad \min \quad & \theta_1 \sum_{j \in J} \sum_{i \in W_j(r)} -\tilde{r}_i^p p_i x_{ij} + \theta_2 \sum_{j \in J} \tilde{r}_j^s q_j y_j + \theta_3 \sum_{j \in J} \sum_{i \in W_j(r)} \tilde{r}_{ij}^e p_i x_{ij} & (1a) \\
\text{s.t.} \quad & \sum_{i \in W_j(r)} p_i x_{ij} \leq q_j y_j, \quad j \in J & (1b) \\
& \sum_{j \in V_i(r) \cap J} x_{ij} \leq 1, \quad i \in I & (1c) \\
& \sum_{j \in J} c_j y_j \leq B & (1d) \\
& x_{ij} \geq 0, \quad i \in I, j \in J & (1e) \\
& y_j \in \{0, 1\}, \quad j \in J. & (1f)
\end{aligned}$$

The objective (1a) consists of minimizing the total risk consisting of the population risk (first term), the shelter risk (second term), and the evacuation risk (third term). θ_1 , θ_2 , and θ_3 represent the weights associated with each term. Constraints (1b) impose the maximal shelter capacity. Constraints (1c) ensure that the number of people assigned from population point i does not exceed its population in need of shelter, i.e., the proportion is at most one. Constraint (1d) impose the maximal budget B to locate new shelters. Constraints (1e) and (1f) define the variable domain.

4 Risk identification and assessment

Uncertainty refers to situations involving imperfect or unknown information and is typically quantified using probability functions (Dönmez et al., 2021). Disasters are characterized by multiple uncertainties, which encompass not only their sources but also their highly erratic potential impacts over time. Neglecting to account for uncertainty in decision-making can lead to inefficient solutions. However, when predicting disasters that have not yet occurred, especially those with low-probability high-consequence outcomes, there is no historical distribution of previous events from which to extrapolate. Even for more frequently occurring disasters in some areas, including floods, it is essential to assess whether the background conditions under which past events were recorded have remained stable or changed, possibly due to climate or socio-economic changes. In such circumstances, probabilities cannot be precisely calculated but have to be estimated (Eiser et al., 2012). While stochastic programming offers an efficient framework for optimizing problems involving uncertainty (Birge and Louveaux, 2011), it assumes a priori knowledge of the probability distributions of uncertain parameters, often represented by discrete realizations as approximations to real probability distributions. This representation of uncertainty may not be suitable for shelter network design in flood-prone areas in developing countries with limited historical data. One potential solution for addressing disaster-related uncertainty is to incorporate risk measures into the parameterization of an optimization model.

This implies that risk must be assessed and measured for the elements of the graph representing the network to be optimized (e.g., population points, shelter locations and infrastructure, as well as evacuation paths).

Risk assessments span a wide and multidisciplinary research field with different views on how to systematically address risk (INFORM, 2016). In the literature, frameworks and analytical models of varying complexity have been proposed at different levels (Cardona et al., 2012), for example, indicator-based global assessments, such as the INFORM Risk Index (INFORM, 2016), and qualitative participatory approaches at the local level, such as a risk reporting process conducted in an enterprise (e.g., Walmart’s risk management program). Risk assessment is a process that aims to systematically identify, analyze, and evaluate potential threats that could have adverse consequences on an entity to enable effective management of uncertainty and inform decision-making. It relies on a rigorous understanding of the determinants of risk and the appropriate measurement of these determinants. This section aims to provide such an understanding by discussing the important elements to take into consideration when evaluating these determinants used to measure the risk associated with shelter networks in flood-prone areas.

The importance of considering risks in disaster management is acknowledged in the literature (Heckmann et al., 2015; Steelman and McCaffrey, 2013). Risk analysis allows for the identification of the locations and population most likely to be affected by potential disasters, thereby assisting in managing preparedness and response to humanitarian crises (Marin-Ferrer et al., 2017). While there is no universally accepted definition of risk (Thompson et al., 2016), disaster risk is widely understood as the result of the interaction between a hazard and the characteristics that make some locations vulnerable and exposed (McGlade et al., 2019). In the literature, many authors (Arnette and Zobel, 2019; Cardona, 2004; Heckmann et al., 2015; Merz et al., 2013) defined risk as:

$$Risk = Hazard \times Vulnerability \times Exposure,$$

where *hazard*, *vulnerability*, and *exposure* are the main determinants of risk (United Nations, 2016). These determinants are defined and discussed below. The advantage of such formulation is to incorporate not only the likelihood and severity of a disaster, but also the characteristics of the affected population, buildings, and infrastructures that could be impacted by such an event.

Hazard The United Nations define hazard as “a process, phenomenon or human activity that may cause loss of life, injury or other health impacts, property damage, social and economic disruption or environmental degradation” (United Nations, 2016). Similar definitions are also generally used in the scientific literature (Arnette and Zobel, 2019; Akgün et al., 2015; Cardona, 2004; Thompson et al., 2016). In the context of floods, the probability of occurrence of flood (see Arnette and Zobel, 2019) and the flood water level (see Tran et al., 2009) have been used as estimates of hazard. Therefore, water depth in the event of a flood (referred to as flood depth) is an appropriate predictor of hazard in a specific location. However, estimating flood depth is not trivial and requires processing a large amount of data, including rainfall, water levels, water quantity, terrain elevation, and flood occurrences. Various estimates have been proposed (see Cohen et al., 2019; FEMA, 2023; Teng et al., 2022, for examples), and high-resolution flood hazard maps, obtained using the outputs of complex flood models, provide valuable flood hazard estimates. In the case of Haiti, we benefit from such a high-

resolution map that allowed the extraction of geolocalized flood depth indicators obtained through a reliable flood model (namely, HEC-RAS) and inputs (Heimhuber et al., 2015; World Bank, 2023).

Vulnerability The United Nations define vulnerability as “the conditions determined by physical, social, economic and environmental factors or processes which increase the susceptibility of an individual, a community, assets or systems to the impacts of hazards” (United Nations, 2016). It can be seen as an internal risk factor and expressed by how the system will be affected by the hazard (Cardona, 2004; Heckmann et al., 2015; Thompson et al., 2016). Within the context of disaster risk management, vulnerability indices have been used to measure the vulnerability of the different components of the system. These indices consider factors that determine the ability to resist and recover from the impacts of a disaster. One of the most common indices is related to social vulnerability which usually considers demographic and socioeconomic characteristics, health, coping capacity (e.g., housing conditions), and environmental factors (Alem et al., 2021; Arnette and Zobel, 2019; Rufat et al., 2015; Tran et al., 2009). Vulnerability indices for buildings usually include its ability to resist and recover from the impacts of a disaster. A few measures have been proposed for specific disasters such as earthquakes (Kassem et al., 2019) and wildfires (Papathoma-Köhle et al., 2022), and for specific regions such as the European Alps (Papathoma-Köhle et al., 2019). In the context of flood-prone areas, it is important to estimate the vulnerability of the population as well as the infrastructure (e.g., shelters). In the case of Haiti, we benefit from a Wealth Index that accounts for several social vulnerability drivers derived by the World Bank in Haiti as well as a vulnerability index for shelter that accounts for their year of construction also provided by the World Bank.

Exposure The United Nations define exposure as “the situation of people, infrastructure, housing, production capacities and other tangible human assets located in hazard-prone areas” (United Nations, 2016). The exposure does not depend on the vulnerability and susceptibility to the potential damages of a disaster (Bhamra et al., 2011; Johnston et al., 2020; Miller and Ager, 2012; Turner et al., 2003), but rather on the degree, duration or extension of the system’s contact with the hazard (Akgün et al., 2015; Arnette and Zobel, 2019; Thompson et al., 2016; Tran et al., 2009). Therefore, the exposure of a system to a flood can be estimated by determining the extent to which the components of this system are susceptible to being submerged by water. For example, for buildings such as shelters, two important elements to consider are the size of the building and whether it is located in a flood-prone area. A larger shelter will be more exposed to the same flood as a smaller shelter due to its size (area in contact with the flood). The flood area, measured in square meters, can be used as an indicator of exposure, and an area will be considered as flooded if its flood depth is larger than zero. In the case of Haiti, as for hazard, we benefit from the outputs of flood maps to estimate such exposure drivers in our area of interest, and this is done at a small aggregation level.

Defining risk as a function of these determinants (i.e., hazard, vulnerability, and exposure) allows to distinguish the external risk factors that are not really influenceable (e.g., natural hazards) from internal risk factors that can be somewhat controlled (e.g., limiting the impacts of a natural hazard through robust infrastructure) (Birkmann, 2006). Hence, risk arises from the interplay of uncontrollable external factors and the intrinsic characteristics of the system (Heckmann et al., 2015). Hazard, vulnerability, and exposure mutually influence risk, and none of these elements can be considered in isolation. In the absence of a hazard, defining vulnerability to potential damages becomes meaningless. Similarly, a situation cannot be classified as a hazard for a system if it lacks both exposure and

vulnerability to a potential event ([Cardona et al., 2012](#); [Kron, 2005](#)).

In Section 5, we provide a detailed description of how we overcame the challenges related to data availability to measure risk in the case of Haiti, utilizing different data sources at a small level of geolocalized aggregation.

5 Data collection, processing and description in Haiti

The main goal of this study is to improve the shelter location process by providing a systematic tool that considers risk to guide the Government of Haiti as well as its funding partner, i.e., the World Bank. In existing work on facility location under uncertainty focusing on humanitarian settings, the main sources of uncertainty can be categorized under the three following components of a network: demand (i.e., the needs and locations of people affected), supply (i.e., availabilities at facilities involved in offered relief services), and network connectivity (i.e., conditions of the transportation links) ([Dönmez et al., 2021](#)). In our context, this categorization can be translated into risk experienced at three components of a shelter network: population (demand), shelter (supply), and evacuation path (network). For each of these components, we have clarified the main goals, and identified operational constraints and standards in coverage of vulnerable populations.

Most of the data needed to capture the main elements of the problem under study have a spatial component, which represents an opportunity to use GIS ([Mansourian et al., 2006](#); [Nedović-Budić and Pinto, 1999](#)). In fact, we have seen a significant increase in the application of GIS for modelling humanitarian logistics in recent years. Some studies related to OR/MS approaches that specifically dealt with the shelter location problem have incorporated their models with GIS. These applications range from using GIS databases for numerical analysis ([Alçada-Almeida et al., 2009](#); [Dalal and Üster, 2018](#); [Kongsomsaksakul et al., 2005](#)), to visualizing solutions via color-coded GIS maps ([Chen et al., 2013](#); [Coutinho-Rodrigues et al., 2012](#); [Kılıcı et al., 2015](#)), identifying candidate shelter locations ([Chanta and Sangsawang, 2012](#)), obtaining road network distances, generating matrices of accessibility, and performing network analyses ([Coutinho-Rodrigues et al., 2012](#); [Hallak et al., 2019](#); [Rodríguez-Espíndola and Gaytán, 2015](#)). In the specific context of flood disaster, [Chang et al. \(2007\)](#) used GIS to estimate the location of demand points and the quantities of required rescue equipment under different rainfall situations. [Rodríguez-Espíndola and Gaytán \(2015\)](#) employed raster GIS, which divides a study area into a regular grid of cells, each containing a single value, to create flood scenarios and identify water level in each scenario. [Rodríguez-Espíndola et al. \(2016\)](#) extended the procedure described by [Rodríguez-Espíndola and Gaytán \(2015\)](#) and introduced a method as a combination of raster and vector GIS. As opposed to raster GIS, vector GIS uses discrete line segments and points to represent locations, and can represent points, lines, and areas ([Church, 2002](#)). In [Rodríguez-Espíndola et al. \(2016\)](#), vector GIS was used for data pre-processing and post-analysis, and raster GIS for analyzing potential flooding scenarios. Building upon [Rodríguez-Espíndola and Gaytán \(2015\)](#), [Rodríguez-Espíndola et al. \(2018\)](#) used vector GIS to locate suitable facilities and perform network analysis and raster GIS to consider different scenarios, discard facilities prone to flooding, and identify road failures.

In this study, we have collected reliable data such as geospatial information, high-resolution flood hazard maps, and socio-demographic information in order to properly parametrize the RB-SLP. These data included publicly available data from the World Bank and OpenStreetMap, as well as data ob-

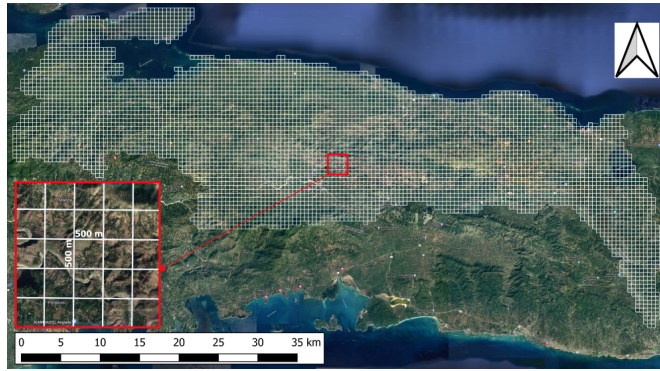


Fig. 2: Satellite image divided into 500 m \times 500 m grids

tained through extensive discussions and interviews with different experts from the World Bank and the Government of Haiti. More precisely, we obtained GIS data from the World Bank which contained four layers: a *flood layer*, a *population layer*, an *existing shelter layer*, and a *new potential shelter layer*. The first layer is raster GIS, while the other three layers are vector GIS. Because raster GIS divides the study area into a regular grid of cells, with each cell (or pixel) containing a single value, while vector GIS uses polygons, discrete line segments, and points to represent locations (Church, 2002), the data were overlapped to conduct “zonal statistics”, thereby requiring extensive data processing. Note that we refer to a pixel in the GIS layer as a surface of 10m \times 10m and a grid as a surface of 500m \times 500m. The satellite image of the Nippes is shown in Fig. 2 along with the grid used to divide the region. In order to make network design, we discretize the continuous space of the Nippes and aggregate data using grids.

In the following, we describe the data collected as well as the data processing. We first describe the *flood layer*, i.e., a flood hazard map. Then, we discuss the data related to the three components of a shelter network: population, shelters, and evacuation paths. For each, we also propose a risk measure. Each risk measure has also been normalized by using standard methods considering the interquartile range (IQR) and winsorizing to handle outlier values and then scaled to a [0,1] range (see Appendix B for detailed information). While our methodology is developed and tested using data from the Nippes Department of Haiti, it can also be implemented for any other flood-prone areas in the world.

5.1 Flood hazard map

A flood hazard map, referred to as the *flood layer*, was modelled by the World Bank team using the Hydrologic Engineering Center’s River Analysis System (HEC-RAS) V5.0.6 (World Bank, 2019b). HEC-RAS allows to perform one-dimensional steady flow, one- and two-dimensional unsteady flow calculations, sediment transport or mobile bed computations, as well as water temperature and water quality modeling (U.S. Army Corps of Engineers Hydrologic Engineering Center, 2023). In this layer, the flood depth (in meters) is available for each pixel. If the flood depth takes a positive value, then that pixel is said to be flooded. Figure 3 presents a map of the flood depth and flood area for the Nippes Department of Haiti, where the flood depth is measured in meters and the flood area is measured as the percentage of flooded pixels. For readability purposes, the data are aggregated in grids which are classified in four categories based on the classification used by the World Bank: i) safe zones with a flood area of at most 20% and flood depth of at most 2 meters; ii) low hazard zones with a flood area of at most 20% and flood depth of more than 2 meters; iii) medium hazard zones

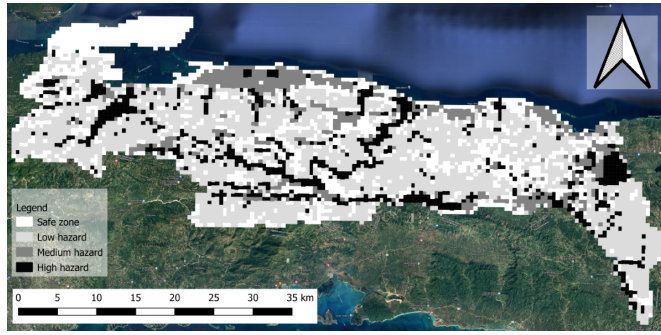


Fig. 3: Classification of flood hazard zone in Nippes

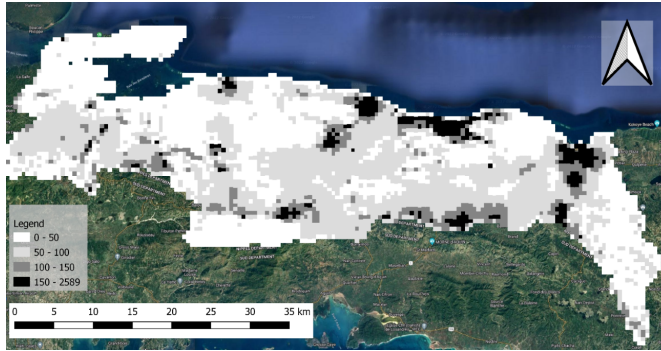


Fig. 4: Population of grids (population points) in Nippes

with flood area of more than 20% and flood depth of at most 2 meters; and iv) high hazard zones with a flood area of more than 20% and flood depth of more than 2 meters.

5.2 Population data and risk assessment

In the following, we provide information about the specific population data provided by the World Bank, referred to as the *population layer*. Then, using that data, we detail how we have obtained the specific population parameters that are found in our mathematical formulation, that is, the population in need of shelter (p_i) according to the population data. Finally, using the *population layer* and the *flood layer*, we explain how risk is assessed and measured for every population point (r_i^p).

Population layer (vector GIS). Specific data about population points, including the population and the wealth index of the population, were provided by the World Bank in the *population layer* (vector GIS). This layer was discretized in grids, for a total of 5,331 grids. Each grid was then associated with exactly one population point (i.e., $|I| = 5,331$), and each population point i is located in the centroid of its associated grid. The data (population and wealth index) was then aggregated for each grid. The total population of Nippes is 347,461 people, and Figure 4 presents the grids (i.e., one grid is one population point) classified according to their population. The wealth index was specifically developed by the World Bank team for Haiti and considers three elements: (i) the physical assets (i.e., ownership of motorized means of transportation, durable goods, productive goods, and housing conditions); (ii) the human capital (i.e., education and health); and (iii) the financial assets (i.e., having a bank account). Figure 5 classifies the grids based on the wealth index, with higher values indicating greater wealth. This classification reveals that the western part of the Nippes Department has the lowest household wealth.

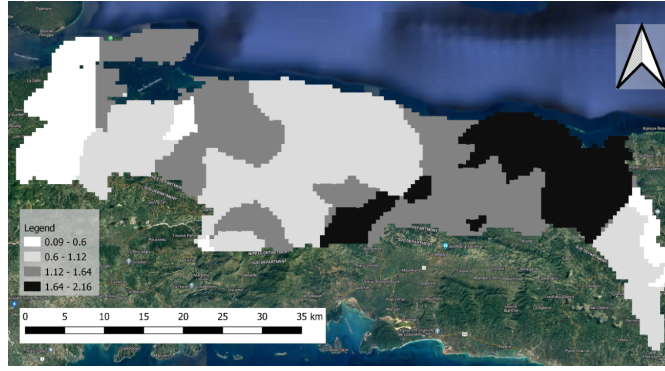


Fig. 5: Wealth index of grids (population points) in Nippes

Population in need of shelter ($p_i, i \in I$). To determine the population in need of shelter, we conducted discussions with the H-SDRMCRP team who confirmed that only a small percentage of affected people evacuate toward shelters while others seek refuge in different places. This is common in case of emergency where there are usually three groups (Cova et al., 2011): (i) those who leave early and travel to a location outside the danger zone; (ii) those who decide to shelter in refuge within the danger zone; and (iii) those who decide to stay at their houses (i.e., shelter-in-place). Therefore, the population in need of shelter, differed from the total population and had to be estimated. While there is no specific data for this in Haiti, different values have been used in the literature to determine the percentage of people which will evacuate toward shelters, e.g. Arnette and Zobel (2019) proposed a range between 2% and 50% and a fixed value of 14.7%, while Kilci et al. (2015) used a fixed value of 12.5%. Mileti et al. (1992) found that when expert opinion is unavailable and there is insufficient historical data, then the constant sheltering need of 14.7% across all locations still provide a reasonable outcome. Therefore, in this paper, we consider a constant sheltering need of 14.7% in all grids, i.e., $p_i = 0.147 \times p'_i, \forall i \in I$, where p'_i is the total population of i .

Population risk assessment ($r_i^p, i \in I$). In accordance with the definitions of hazard, vulnerability, and exposure provided in Section 4, the population risk r_i^p of each population point $i \in I$ is computed as

$$r_i^p = (f_i^d) \times (v_i^p) \times (f_i^a \times (1 - \tilde{p}_i/p_i)), \quad (2)$$

where f_i^d , the flood depth of population point i , represents hazard; v_i^p , the social vulnerability index of population point i , represents vulnerability; and f_i^a , the flood area of population point i , multiplied by $(1 - \tilde{p}_i/p_i)$, the percentage of uncovered people from population point i with existing shelters, represents exposure.

To determine the flood depth and flood area of each population point, we conducted “zonal statistics” by overlapping the *flood layer* with the *population layer*. We then obtained, for each grid, its average flood depth as well as the number of flooded pixels. Therefore, the flood depth of population point i (f_i^d) is set to the flood depth of its associated grid, and the flooded area of population point i (f_i^a) is calculated by multiplying the percentage of flooded pixels in its corresponding grid by the grid’s area, which is 500m x 500m.

To determine a social vulnerability index, we determined that the inverse of the wealth index is a good estimate for the social vulnerability index because it includes the key factors of social vulnerability,

that is, (i) demographic characteristics, (ii) socioeconomic status, (iii) health, (iv) coping capacity, and (v) environmental factors (see Rufat et al., 2015). Therefore, the social vulnerability index of each population point is computed as

$$v_i^p = \frac{1}{w_i},$$

where w_i represents the wealth index of population point i .

To determine the percentage of uncovered people with existing shelters, the value of \tilde{p}_i was determined by solving a mathematical model (Model 3) that assigns the population in need of shelter to existing shelters (J') by minimizing the total risk. Appendix A presents additional details including this mathematical model.

Table 1 summarizes the data for the population points. The data related to the population points has a high variability, especially for the population, the flood area and the population risk.

Table 1 Summary of the population data ($i \in I$)

Data	Notation	Average	Std. Dev.
Population in need of shelter	p_i	10.1	11.3
Flood depth (m)	f_i^d	1.9	0.8
Flooded area (m ²)	f_i^a	45,314.7	55,480.2
Social vulnerability index	v_i^p	1.4	1.4
Percentage of uncovered people in the existing network	$1 - \tilde{p}_i/p_i$	87.1	33.4
Population risk	r_i^p	59,452.5	62,848.4
Normalized population risk	\tilde{r}_i^p	0.3	0.3

5.3 Shelter data and risk assessment

In the following, we provide information about the specific shelter data provided by the World Bank, referred to as the *existing shelter layer* and the *new potential shelter layer*. Then, using that data, we detail how we have obtained the specific shelter parameters that are found in our mathematical formulation, that is, the maximal shelter capacity (q_j), the cost of locating a shelter (c_j), the maximal coverage radius (r), and the maximal budget (B). Finally, using the *existing shelter layer*, the *new potential shelter layer* and the *flood layer*, we explain how risk is assessed and measured for every shelter (r_j^s).

Existing shelter layer and new potential shelter layer (vector GIS). The specific data related to the shelters were provided by the World Bank and contained two layers (vector GIS): the *existing shelter layer* and the *new potential shelter layer*. The *existing shelter layer* contains data about the size and location of the existing shelters J' . The existing shelters comprise public buildings such as schools, auditoriums, and churches, which are primarily used for purposes other than sheltering. These buildings, not constructed according to current building codes, are more vulnerable to disasters and lack necessary sheltering infrastructure, such as appropriate utility spaces including kitchens and toilets. In addition, using these buildings for medium or long-term sheltering is not ideal, as it would require stopping their primary activities. While we refer to these buildings as existing shelters for readability purposes, it would be more appropriate to refer to them as “potential existing shelters” or as “public buildings”. The *new potential shelter layer* contains data about the location of new

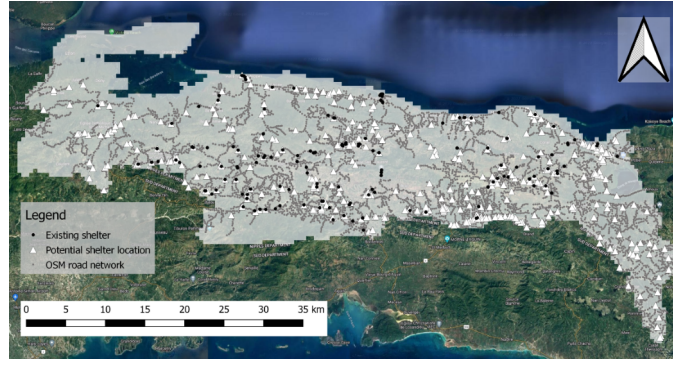


Fig. 6: Set of potential shelter locations J and existing shelters J' in Nippes

potential shelters J . The Government of Haiti in partnership with the World Bank decided to locate new potential shelters in the premises of existing public schools with road accessibility within 150 meters. Figure 6 shows the location of the 349 potential shelter locations and 144 existing shelters in Nippes Department. The map shows that many existing shelters, being inaccessible by road, are effectively unusable for sheltering needs.

Shelter capacity ($q_j, j \in J \cup J'$). To determine the capacity of new potential shelters $q_j, j \in J$, government standards are used. The government imposes an area (living space) of 300 square meters per shelter, and we denote by s_j the size (living space in square meters) of the shelter, i.e., $s_j = 300, j \in J$. In addition, these standards also impose a living area of 3 square meters per person which limit the capacity of each new potential shelter to 100 people ($q_j = 100, j \in J$). For existing shelters, as previously explained, their size $s_j, j \in J'$ is available in the *existing shelter layer* data. Using the same government standards for the living area, we set the capacity of existing shelters to $q_j = \lfloor s_j/3 \rfloor, j \in J'$.

Cost of locating a shelter ($c_j, j \in J$). Our partners estimated that the cost of locating (building) a new shelter is 560,000 US dollars ($c_j = 560,000, \forall j \in J$). This cost represents the construction cost of a shelter and includes a fixed construction cost, as well as variable costs for land ownership, type of soil, and type of region.

Coverage radius (r). The maximal coverage radius needed to satisfy standards targeted by the government. In addition, it needed to allow foot-based evacuations. Therefore, after discussions with the H-SDRMCRP team, the maximal coverage radius of shelters was set to 3 km ($r = 3$), that is, only population points within a Euclidean distance of 3 km can be covered from a given shelter.

Budget (B). Given the H-SDRMCRP project appraisal document's budget (World Bank, 2019a), i.e., 35 million US dollars equally divided by 5 departments, a budget of 7 million US dollars ($B = 7,000,000$) was defined to build shelters in Nippes Department. This is an upper bound as it excludes unpredictable and fluctuating costs like training, field work, and logistics, which are inherent to the project. Therefore, given the estimated construction cost ($c_j = 560,000, \forall j \in J$), at most 12 new shelters can be built in the department.

Shelter risk assessment ($r_j^s, j \in J \cup J'$). According to the definitions of hazard, vulnerability, and exposure provided in Section 4, the shelter risk r_j^s of each shelter $j \in J \cup J'$ was computed as

$$r_j^s = (f_j^d) \times (v_j^s) \times (f_j^a \times s_j). \quad (3)$$

where f_j^d , the flood depth of shelter j , represents hazard; v_j^s , the vulnerability index of shelter j , represents vulnerability; and f_j^a , the flooded area of shelter j multiplied by s_j , the size of shelter j , represents exposure.

To compute the flood depth and flooded area of each shelter, square buffers were defined in the *existing shelter layer* and the *potential new shelter layer* around each shelter in order to cover its entire area. The length of the side of this square buffer was computed as the square root of the area of the shelter and rounded up to its nearest integer, i.e., $\lceil \sqrt{s_j} \rceil, j \in J \cup J'$. By overlapping the *flood layer* with both the *existing shelter layer* and the *potential new shelter layer*, we obtained, for each shelter's surrounding square buffer, the average flood depth as well as the number of flooded pixels which was converted as a percentage of flooded pixels. Therefore, the flood depth of shelter j (f_j^d) was set as the flood depth of its corresponding square buffer, and the flooded area of shelter j (f_j^a) was computed by multiplying its corresponding buffer's percentage of flooded pixels with the area of the buffer (i.e., $\lceil \sqrt{s_j} \rceil^2, j \in J \cup J'$).

To determine the vulnerability index of each shelter, many discussions were conducted with the H-SDRMCRP team. The team confirmed that the new shelters will be constructed in compliance with the current government standards and construction codes, significantly reducing their vulnerability compared to existing shelters that do not meet these codes and are highly susceptible to various disasters. Therefore, each new shelter $j \in J$ was assigned a shelter vulnerability index of 0.1 ($v_j^s := 0.1$). In the *existing shelter layer* data, the age of each shelter was documented, indicating whether it was new or old. The H-SDRMCRP team determined that a building's age (new or old) served as a proxy for assessing the quality of its infrastructure and its vulnerability. Consequently, older existing shelters are more vulnerable than newer existing shelters. Therefore, the shelter vulnerability index ($v_j^s, j \in J'$) are set to 1 for older existing shelters, and to 0.5 for newer existing shelters.

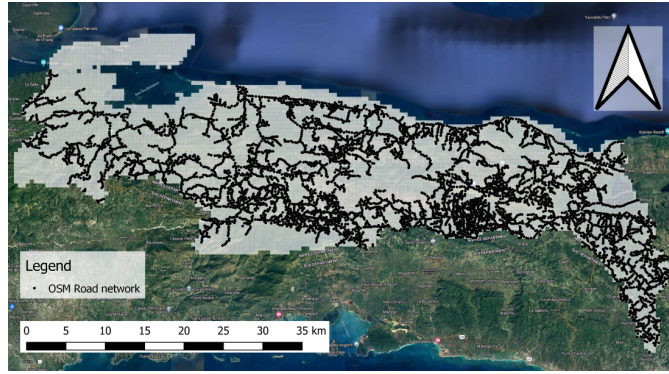
Table 2 summarizes the data for the potential shelter locations and the existing shelters. Note that we present the flooded area as a percentage because the size of existing shelters vary, and it is easier to understand which shelters are in higher flood-prone areas than others. We do not present the shelter capacity and the vulnerability index for the potential shelter locations as all new shelters have a capacity of 100 people and a vulnerability index of 0.1. In addition, many existing shelters do not have road accessibility. The data shows a higher flood depth and flooded area for potential shelter locations than for existing shelters, but the methodology allows to determine where to locate the new shelters.

5.4 Evacuation path data and risk assessment

In the following, we provide information about how we have used OpenStreetMap (OSM) to obtain a real-road network. Then, we detail how we have obtained the specific evacuation parameters that are found in our mathematical formulation, that is, how the travel distance of each edge has been computed ($d_{ij}, (i, j) \in E$). Finally, using the real-road network connected with our GIS data, we

Table 2 Summary of the shelter data

Data	Notation	Average	Std. Dev.
Potential shelter locations $j \in J$			
Flood depth (m)	f_j^d	1.4	0.9
Flooded area (%)	f_j^a	26.7	36.7
Shelter risk	r_j^s	23.4	32.9
Normalized shelter risk	\tilde{r}_j^s	0.3	0.4
Existing shelters $j \in J'$			
Capacity (# people)	q_j	104.0	121.4
Flood depth (m)	f_j^d	0.2	0.5
Flooded area (%)	f_j^a	12.6	30.3
Vulnerability index	v_j^s	0.7	0.3
Shelter risk	r_j^s	21.9	80.4
Normalized shelter risk	\tilde{r}_j^s	0.1	0.2

Fig. 7: OSM network $\mathcal{G} = (\mathcal{N}, \mathcal{A})$

explain how risk is assessed and measured for each path of network (r_{ij}^e).

Real-road network data. To determine the real-road distances, OSM was used. OSM has been shown to be a good tool in environments with limited data (see Sokat et al., 2018, for a framework on data estimation). From OSM, a road-network consisting of single points and space, and road segments was extracted. Figure 7 illustrates the road network of Nippes which consists of 6,359 nodes and 7,351 arcs. Note that this data was converted as GIS vector data, referred to as the *OSM data*. This data was then connected with our network comprising population points and shelters to build a *road layer*. This required extensive data processing (see Appendix C for details).

Travel distance ($d_{ij}, (i, j) \in E$). As detailed in Section 5.3, the H-SDRMCRP team determined that shelters should cover population points within a radius of 3 km measured in Euclidean distance ($r = 3km$), as it allowed to take into account that people could walk on roads as well as off-road to reach a shelter. Therefore, to compute $d_{ij}, (i, j) \in E$, the latitude and longitude of each population point (i.e., the centroid of its grid) and each shelter was extracted from the *population layer*, *existing shelter layer* and *new potential shelter layer*. Recall that d_{ij} is only used to determine to sets of population points that can be covered by shelters.

Evacuation risk assessment ($r_{ij}^e, i \in I, j \in J \cup J'$) Second, by using the concepts of hazard, vulnerability, and exposure provided in Section 4, the evacuation risk represents the difficulty of travelling from one location to another following a flood. More precisely, the evacuation risk between

population point $i \in I$ and shelter $j \in J \in J'$ is computed as

$$r_{ij}^e = t_{ij}, \quad (4)$$

where t_{ij} represents the time to travel (exposure and vulnerability) from population point i to shelter j according to the flood water level (hazard) in the real-road network.

Determining the value of t_{ij} required extensive data processing. To determine the speed of walking in flooded areas, many laboratory experiments have been conducted in open channels (see e.g., Bernardini et al., 2020; Bernardini and Quagliarini, 2020) or pools (see e.g., Lee et al., 2019). On the other hand, these studies focus on flood depths with a maximum of 70 cm. By analyzing the data contained in the provided *flood layer*, we can see that many areas have a flood depth or more than 70 cm with a maximum flood depth of 2.5 meters (see Figure 3). Due to the dearth of studies with a flood depth of more than 70 cm, we computed the evacuation speed based on the experimental study of Bernardini et al. (2020). Given that evacuation speed, we can then compute the shortest-path in terms of evacuation time, denoted by t_{ij} , between each population point $i \in I$ and shelter $j \in J \cup J'$ in the *road layer*. Appendix D presents more details on how the evacuation speed based on Bernardini et al. (2020) was computed.

Table 3 summarizes the evacuation data. The data presents the number of accessible shelters (new potential shelters and existing shelters) within the coverage radius ($r=3\text{km}$) of population points. The data shows that there are more potential new shelter locations within the coverage radius of population points, than existing shelters. In addition, there is a higher evacuation risk to potential new shelters compared with existing shelters which can be explained by the fact that the location of the potential new shelters can be in higher flood-prone areas.

Table 3 Summary of the evacuation data

Data	Notation	Average	Std. Dev.
# of accessible potential new shelter locations	$ V_i(r) \cap J , i \in I$	6.5	4.5
# of accessible existing shelters	$ V_i(r) \cap J' , i \in I$	2.8	3.2
Evacuation risk to new potential shelters	$r_{ij}^e, i \in I, j \in V_i(r) \cap J$	1.7	1.3
Evacuation risk to existing shelters	$r_{ij}^e, i \in I, j \in V_i(r) \cap J'$	1.6	1.2
Normalized evacuation risk to new potential shelters	$\tilde{r}_{ij}^e, i \in I, j \in V_i(r) \cap J$	0.4	0.3
Normalized evacuation risk to existing shelters	$\tilde{r}_{ij}^e, i \in I, j \in V_i(r) \cap J'$	0.3	0.3

6 Computational results and analyses

In this section, we conduct thorough computational analyses to derive appropriate managerial insights. Our model was coded in Python and solved with Gurobi 9.0.2. All the solutions were obtained within five seconds of computational time. First, we solve our problem with different weight settings to analyze their impacts on the solution. Second, using only the weight-vector setting where $\theta_1 = \theta_2 = \theta_3 = 0.33$, we compare our solution with an alternative solution approach, which relies on a typical shelter location problem where the objective function aims to maximize the number of covered people. Third, we conduct sensitivity analysis on the shelter construction cost. Finally, we compare our solution with the one provided by the H-SDRMCRP team and the Government of Haiti. Note that

in all our tables, for a solution, we denote its average normalized population risk as PR, its average normalized shelter risk with SR, and its average normalized evacuation risk with ER. In addition, we denote the percentage of the covered population with new and existing shelters with % Pop. To obtain this value, we first solve Model 1 which only considers the new potential shelters. Then, we solve Model 3 which only considers the existing shelters, but this time only taking into account the population that is not covered with the new shelters obtained by solving Model 1. Therefore, % Pop corresponds to the sum of the covered population obtained in these two steps.

6.1 Analysis of the weights given to the population risk, shelter risk, and evacuation risk

In this section, we present a detailed analysis on the impact of the weight-vector settings $(\theta_1, \theta_2, \theta_3)$ on the solution. While working on this project, the COVID-19 pandemic and the inflation it has caused on construction costs have led to variation with respect to the cost of locating shelters (c_j). In our model, while the initial estimated shelter construction cost and budget ($c_j = 560,000, \forall j \in J$ and $B = 7,000,000$) allowed for the building of 12 new shelters, our partners ended up recommending to test the model with 6 new shelters due to an increase in costs. Therefore, in this section, we discuss the impacts of the weight-vector settings according to different number of new shelters. Our methodology was tested using different values between 6 and 12 new shelters, and our results remained consistent, i.e., the choice of weight-vector was consistent to the number of shelters. For conciseness reasons, we only present the results with 6 and 12 new shelters. The weight-vector settings are classified in two categories: i) extreme weight-vector settings where at least one weight is equal to 0; and ii) non-extreme weight-vector settings where all weights are greater than 0. Note that when setting $\theta_1 = 0$, constraints 1b and 1d are modified to impose equality as otherwise no population points are assigned. In Table 4, we first report the tested weight-vector settings $(\theta_1, \theta_2, \theta_3)$. Then, we present the PR, SR, ER, % Pop.

On the one hand, the results indicate that regardless of the weight-vector setting, the percentage of the population in need of shelter covered by new shelters consistently stands at 1.1% with 6 new shelters and 2.2% with 12 new shelters. This is due to the maximal shelter capacity (i.e., 100 people per shelter), which is always reached. On the other hand, % Pop varies because the percentage of the covered population with existing shelters does. In fact, when solving the risk-based model using existing shelters (Model 3), putting more weight on population risk results in the selection of riskier shelters, consequently covering a higher percentage of the population. Therefore, while the existing shelter capacity could cover 14,439 people, the average is 10,351 people. Note that a large portion of the population in need of shelter (more than 70%) remains uncovered, as many grids either lack a public school with road accessibility or have no existing shelters within a 3 km radius. This does not imply that people could not walk more than 3 km in practice to reach a shelter. Instead, it indicates that in our shelter network design, people are considered covered only if there is a shelter located within a 3 km radius.

Second, by analyzing the three risk measures obtained with the different weight-vector settings, their performance is less variable for the non-extreme weight-vector settings. With 12 shelters, the population, shelter and evacuation risks have an average of 0.99, 0.01, and 0.07 with a standard deviation of 0.01. On the contrary, when considering extreme weight-vector settings with 6 shelters, then the solutions can have higher values of risk which can reach 0.19, 0.44, and 0.30 for the population, shelter

Table 4 Average normalized values with different weight-vector settings with 6 and 12 shelters

Weight-vector setting ($\theta_1, \theta_2, \theta_3$)	6 shelters				12 shelters			
	PR	SR	ER	% Pop	PR	SR	ER	% Pop
Non-extreme weight-vector settings								
(0.15, 0.15, 0.70)	0.98	0.05	0.04	11.4	0.97	0.03	0.05	12.5
(0.15, 0.30, 0.55)	0.98	0.00	0.06	12.4	0.98	0.02	0.06	13.5
(0.15, 0.45, 0.40)	0.98	0.00	0.06	13.3	0.98	0.00	0.07	14.4
(0.30, 0.60, 0.10)	0.99	0.00	0.07	18.3	0.99	0.00	0.09	19.4
(0.33, 0.33, 0.33)	0.99	0.00	0.06	16.0	1.00	0.00	0.07	16.5
(0.45, 0.25, 0.30)	1.00	0.00	0.07	19.5	0.99	0.02	0.07	24.0
(0.45, 0.30, 0.25)	1.00	0.00	0.07	19.7	0.99	0.00	0.08	20.7
(0.50, 0.10, 0.40)	1.00	0.03	0.05	24.0	0.99	0.03	0.06	25.1
(0.50, 0.25, 0.25)	1.00	0.00	0.07	21.1	0.99	0.01	0.07	21.9
(0.50, 0.40, 0.10)	1.00	0.00	0.07	20.7	0.99	0.00	0.09	21.7
(0.60, 0.10, 0.30)	1.00	0.03	0.05	26.3	0.99	0.03	0.06	27.0
(0.60, 0.25, 0.15)	1.00	0.00	0.07	23.0	0.99	0.00	0.09	24.2
(0.75, 0.10, 0.15)	1.00	0.00	0.07	27.4	0.99	0.02	0.07	28.4
(0.75, 0.15, 0.10)	1.00	0.00	0.07	27.6	1.00	0.00	0.09	28.7
(0.90, 0.05, 0.05)	1.00	0.00	0.07	27.8	1.00	0.01	0.08	28.9
Average	0.99	0.01	0.06	20.6	0.99	0.01	0.07	21.8
Std. Dev.	0.01	0.02	0.01	5.5	0.01	0.01	0.01	5.6
Extreme weight-vector settings								
(0.30, 0.00, 0.70)	0.99	0.43	0.03	21.4	0.99	0.28	0.05	22.5
(0.30, 0.70, 0.00)	1.00	0.00	0.30	19.4	1.00	0.00	0.25	20.5
(0.45, 0.00, 0.55)	1.00	0.44	0.03	23.6	0.99	0.28	0.04	24.5
(0.60, 0.40, 0.00)	1.00	0.00	0.23	22.0	1.00	0.00	0.23	23.0
(0.75, 0.00, 0.25)	1.00	0.44	0.03	26.8	0.99	0.28	0.05	27.8
(0.90, 0.00, 0.10)	1.00	0.44	0.03	27.7	1.00	0.32	0.05	28.7
(0.90, 0.10, 0.00)	1.00	0.00	0.30	28.1	1.00	0.00	0.25	29.2
(1.00, 0.00, 0.00)	1.00	0.42	0.29	28.1	1.00	0.30	0.18	29.2
(0.00, 1.00, 0.00)	0.54	0.00	0.26	1.1	0.35	0.00	0.18	2.2
(0.00, 0.00, 1.00)	0.23	0.19	0.00	1.1	0.22	0.17	0.01	2.2
Average	0.88	0.24	0.15	19.9	0.85	0.16	0.13	21.0
Std. Dev.	0.27	0.22	0.13	10.4	0.30	0.15	0.10	10.4
Average all	0.95	0.10	0.10	20.3	0.93	0.07	0.10	21.5
Std. Dev. all	0.18	0.18	0.09	7.6	0.20	0.12	0.07	7.7

and evacuation risks. There is also more variability in the results, i.e., with 12 shelters, the population, shelter and evacuation risks have an average of 0.85, 0.16, and 0.13 with a standard deviation of 0.30, 0.15, and 0.10. Therefore, the risk measures obtained with non-extreme weight-vector settings are more consistent.

6.2 Comparison with a standard objective function

One of the most common objective functions considered in humanitarian logistics is to maximize coverage (Gutjahr and Nolz, 2016). This objective is also common in shelter location problem (see Chanta and Sangsawang, 2012; Doerner et al., 2009; Hallak et al., 2019; Salman and Yücel, 2015; Trivedi and Singh, 2020, for a few examples). In our context, this would correspond to maximizing the covered population in need of shelter, and can be modeled as follows:

$$\begin{aligned}
 \text{Model 2} \quad & \max && \sum_{j \in J} \sum_{i \in W_j(r)} p_i x_{ij} && (5a) \\
 & \text{s.t.} && (1b) - (1f). && (5b)
 \end{aligned}$$

In order to assess the value of considering a risk-based model, this section compares our solutions with the corresponding population, shelter, and population risks resulting from solving Model 2. Given the preference of our partners and the results obtained with non-extreme weight vectors, we then compare the results obtained with the weight-vector (0.33, 0.33, 0.33) which was selected for our proposed objective function (1a).

Table 5 Performance of the solutions obtained with 12 shelters and $(\theta_1, \theta_2, \theta_3) = (0.33, 0.33, 0.33)$

Performance indicator	Model 1	Model 2
PR	0.99	0.39
SR	0.01	0.20
ER	0.07	0.17
% Pop	16.5	29.2

Table 5 reports the value of PR, SR, ER, % Pop. Note that when using the objective function (5a), multiple solutions have the same optimal value. However, the results of some analyses showed that the initial solutions obtained by means of Gurobi are similar to the other optimal solutions. Therefore, for conciseness reasons, we only report that solution.

By comparing our risk-based objective function with a traditional covering objective function (Model 2), we observe that the obtained solution allows to greatly reduce all three measures of risk. In fact, with the objective function (5a), we have population, shelter and evacuation risks of 0.39, 0.20, and 0.17 compared with 0.99, 0.01, and 0.07 with our more complex objective function. When analyzing the covered population in need of shelter within 3 km, we cover more people when considering the objective function (5a) (29.2% compared with 16.5%). In addition, for both objective functions, new shelters always cover 2.2% of the population implying that 27.0% of the population is covered with existing shelters using objective function (5a). This can be explained by the fact that upon solving the risk-based model, it is sometimes better not to assign population points to shelters which would be too risky. This issue could be solved by imposing equality in constraints (1b). We can conclude that considering a risk-based objective function is important as it helps to find solutions with a very low risk for each risk measure, compared with a more general approach which does not consider risk at all.

6.3 Impact of the number of shelters

In this section, we analyze the impact on the number of shelters on the three risk measures as well as the percentage of the population covered by new and existing shelters. This analysis is important, because in practice, two things could happen: i) the cost of the shelters c_j might be higher (or lower) than expected; and ii) the available budget B might be higher or lower than expected.

Table 6 Impact of the number of shelters on the average normalized risks obtained with $(\theta_1, \theta_2, \theta_3) = (0.33, 0.33, 0.33)$

# Shelters	PR	SR	ER	% Pop
4	0.99	0.00	0.05	15.6
5	0.99	0.00	0.06	15.8
6	0.99	0.00	0.06	16.0
7	0.99	0.00	0.07	16.2
8	1.00	0.00	0.07	16.4
9	1.00	0.00	0.07	16.6
10	1.00	0.00	0.07	16.8
11	1.00	0.00	0.07	17.0
12	1.00	0.00	0.07	17.1
13	1.00	0.00	0.07	17.3
14	1.00	0.01	0.07	17.5
15	1.00	0.01	0.07	17.7
16	1.00	0.02	0.08	17.9
17	1.00	0.02	0.08	18.1
18	1.00	0.02	0.08	18.3
19	1.00	0.03	0.08	18.4
20	1.00	0.03	0.08	18.6

By modifying constraint (1d) and with $(\theta_1, \theta_2, \theta_3) = (0.33, 0.33, 0.33)$, Table 6 reports for each number of shelters (*# Shelters*) its resulting PR, SR, ER, and %Pop. While one could expect a risk-decrease upon increasing the number of shelters, our results show the opposite. In fact, the trend shows that when increasing the number of new shelters, riskier population is covered, and there is an increase in the shelter and evacuation risks. In particular, by going from 4 to 20 shelters, the population, shelter and evacuation risks go from 0.99 to 1.00, from 0.00 to 0.03, and from 0.05 to 0.08. This is due to two important elements. First, when more shelters are available, a higher population in need of shelter can be covered which results in covering riskier population points. Second, when locating a few number of shelters (e.g., 4), these shelters tend to be located in less risky area and to cover less risky population points thus resulting in a lower shelter and evacuation risks. In general, for all three risk-measures, our solution approach is robust to an increase (or a decrease) on the number of shelters which could be due to a decrease (or an increase) on the construction costs or to an increase (or a decrease) on the available budget. Finally, when increasing the number of new shelters, we increase the population covered by the new shelters and always use the total capacity of these shelters.

6.4 Comparison with our partners' solution

During our work on this project, there was some uncertainty on the final shelter construction cost c_j . Therefore, the H-SDRMCRP team decided to be conservative and select 6 new shelter locations and gave its recommendation to the Government of Haiti. To identify these shelters, the H-SDRMCRP team started spatial assessments in 2019 which were conducted as follows. First, public schools with land availability and road accessibility within 150 meters were identified. Second, for each of these

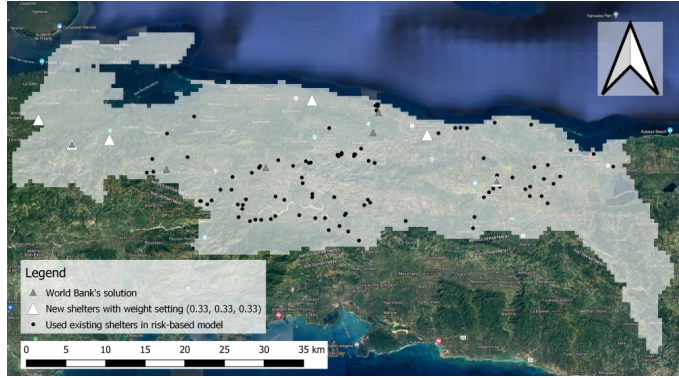


Fig. 8: The H-SDRMCRP team’s solution versus the risk-based model’s solution with (0.33,0.33,0.33)

public schools, the number of existing shelters in a 150-meter radius, the number of people in a 3-km radius, and the number of people living in flood-prone areas in a 3-km radius have been computed. Third, final field visits were conducted to gather more information, and recommendations have been made in order to determine where to locate these new shelters. With these recommendations, the Government of Haiti can analyze the possibility of building the shelters in the selected areas. Therefore, in this section, we compare the solution recommended by our optimization approach (i.e., solving the RB-SLP) with the solution provided by the H-SDRMCRP team. This allows us to determine the importance of developing a sophisticated mathematical model that can consider risk in the objective function in a more holistic way and evaluate all possible alternative as opposed to a more manual process.

Table 7 Performance comparison of our partners’ solution and our approach with 6 shelters $(\theta_1, \theta_2, \theta_3) = (0.33, 0.33, 0.33)$

Performance indicator	Partners	Our
PR	0.64	0.99
SR	0.03	0.00
ER	0.24	0.06
% Pop	28.0	16.0

The solution provided by the H-SDRMCRP team along with our risk-based model’s solution obtained with the weight-vector setting (0.33, 0.33, 0.33) are depicted in Figure 8. Table 7 reports the value of PR, SR, ER, % Pop for these two solutions. In both solutions, the maximum number of people is covered with new shelters, representing 1.1% of the covered population in need of shelter. In addition, our results show that for all risk measures, our solution approach outperforms the solution provided by our partners. This is the most important for the population risk which goes from 0.64 to 0.99, which implies that our solution approach allows to select the population points with the higher risk and assigned them to shelters. The shelter risk also decreases from 0.03 to 0 which implies that less risky shelters are selected. Finally, the evacuation decreases from 0.24 to 0.06 which allows the population to evacuate using safer paths. This shows the effectiveness of our approach.

7 Conclusions

Lack of access to shelters is one of the most important humanitarian and development problems in remote areas of developing countries. Addressing shelter needs during and after a disaster remains a serious challenge for governments and humanitarian agencies. In this paper, we have solved a shelter network design problem motivated by the need to reconstruct the shelter network of flood-prone regions in Haiti. We have proposed a risk-based approach to assess and measure the inherent risks of the shelter network. In particular, three risk measures (population risk, shelter risk, and evacuation risk) have been defined to represent the uncertain nature of demand, supply, and network. As a first attempt to study pedestrian-based evacuation in an optimization model, we have developed a new methodology inspired from empirical research to estimate the risk of evacuation in flood water.

Despite the scarcity of data in the humanitarian sector, we succeeded in gathering data from various sources (e.g., geospatial information, high-resolution flooding maps, socio-demographic data, road network). In particular, our collaboration with the World Bank and the Government of Haiti allowed the formulation of a well-defined and realistic problem, adequately parameterized using real data. This collaboration also allowed us to fully understand the context and determine the decisions, constraints, objectives, and particularities of stakeholders (e.g., Haitian Government) to define and solve the problem.

We have conducted extensive numerical analyses to ensure robustness and correctness, while demonstrating the efficacy of our risk-based methodology. We also proposed different performance indicators adapted for this context that allows to evaluate the solutions on several dimensions. Our results showed that while different solutions are obtained according to the weight given to each risk measure, if we do not use extreme values, our model is robust in terms of solution quality. In addition, by comparing our methodology to a standard methodology where we maximize the covered population in need of shelter and with the current solution of the H-SDRMCRP team, we showed the need for risk-based models.

The solution approach was validated by our partners and our method have been extended to make recommendations on possible shelter locations in another department of Haiti, namely Nord-Ouest Department, which have been used for further field investigation by the Government. This collaboration proved advantageous for our partners as they recognized the approach as an innovative tool that can be applied to different departments and different fields of investment. While we have focused on a particular district of Haiti, the proposed methodology is of general applicability and can be adapted to other regions of the world. This study contributes to the advancement of the UN Sustainable Development Goals 11, 13, and 17, which focus on sustainable cities and communities, climate action, and partnerships for goals.

References

- İ. Akgün, F. Gümüşbuğa, and B. Tansel. Risk based facility location by using fault tree analysis in disaster management. *Omega*, 52:168–179, 2015.
- L. Alçada-Almeida, L. Tralhão, L. Santos, and J. Coutinho-Rodrigues. A multiobjective approach to locate emergency shelters and identify evacuation routes in urban areas. *Geographical Analysis*, 41(1):9–29, 2009.
- D. Alem, H. F. Bonilla-Londono, A. P. Barbosa-Povoa, S. Relvas, D. Ferreira, and A. Moreno. Building disaster

- preparedness and response capacity in humanitarian supply chains using the Social Vulnerability Index. *European Journal of Operational Research*, 292(1):250–275, 2021.
- N. Altay and W. G. Green III. OR/MS research in disaster operations management. *European Journal of Operational Research*, 175(1):475–493, 2006.
- A. E. Amideo, M. P. Scaparra, and K. Kotiadis. Optimising shelter location and evacuation routing operations: The critical issues. *European Journal of Operational Research*, 279(2):279–295, 2019.
- A. N. Arnette and C. W. Zobel. A risk-based approach to improving disaster relief asset pre-positioning. *Production and Operations Management*, 28(2):457–478, 2019.
- O. Arslan, G. Ç. Kumcu, B. Y. Kara, and G. Laporte. The location and location-routing problem for the refugee camp network design. *Transportation Research Part B: Methodological*, 143:201–220, 2021.
- E. J. Baker. Hurricane evacuation behavior. *International Journal of Mass Emergencies & Disasters*, 9(2):287–310, 1991.
- B. Barnes, S. Dunn, C. Pearson, and S. Wilkinson. Improving human behaviour in macroscale city evacuation agent-based simulation. *International Journal of Disaster Risk Reduction*, 60:102289, 2021.
- V. Bayram. Optimization models for large scale network evacuation planning and management: A literature review. *Surveys in Operations Research and Management Science*, 21(2):63–84, 2016.
- V. Bayram and H. Yaman. Shelter location and evacuation route assignment under uncertainty: A Benders decomposition approach. *Transportation Science*, 52(2):416–436, 2018.
- A. Behl and P. Dutta. Humanitarian supply chain management: A thematic literature review and future directions of research. *Annals of Operations Research*, 283(1-2):1001–1044, 2019.
- G. Bernardini and E. Quagliarini. How to account for the human motion to improve flood risk assessment in urban areas. *Water*, 12(5):1316, 2020.
- G. Bernardini, E. Quagliarini, M. D’Orazio, and M. Brocchini. Towards the simulation of flood evacuation in urban scenarios: Experiments to estimate human motion speed in floodwaters. *Safety Science*, 123:104563, 2020.
- G. Bernardini, G. Romano, L. Soldini, and E. Quagliarini. How urban layout and pedestrian evacuation behaviours can influence flood risk assessment in riverine historic built environments. *Sustainable Cities and Society*, 70:102876, 2021.
- M. Besiou and L. N. Van Wassenhove. Humanitarian operations: A world of opportunity for relevant and impactful research. *Manufacturing & Service Operations Management*, 22(1):135–145, 2020.
- M. Besiou, A. J. Pedraza-Martinez, and L. N. Van Wassenhove. OR applied to humanitarian operations. *European Journal of Operational Research*, 269(2):397–405, 2018.
- R. Bhamra, S. Dani, and K. Burnard. Resilience: the concept, a literature review and future directions. *International Journal of Production Research*, 49(18):5375–5393, 2011.
- J. R. Birge and F. Louveaux. *Introduction to stochastic programming*. Springer Science & Business Media, 2011.
- J. Birkmann. Measuring vulnerability to promote disaster-resilient societies: Conceptual frameworks and definitions. In *Measuring vulnerability to natural hazards: Towards disaster resilient societies*, chapter 1, pages 9–54. TERI, 2006.
- C. Boonmee, M. Arimura, and T. Asada. Facility location optimization model for emergency humanitarian logistics. *International Journal of Disaster Risk Reduction*, 24:485–498, 2017.
- O. D. Cardona. The need for rethinking the concepts of vulnerability and risk from a holistic perspective: A necessary review and criticism for effective risk management. In G. Bankoff, G. Frerks, and D. Hillhorst, editors, *Mapping Vulnerability: Disasters, development and people*, chapter 3, pages 37–51. London,UK: Earthscan Publications, first edi edition, 2004.
- O. D. Cardona, M. K. Van Aalst, J. Birkmann, M. Fordham, G. Mc Gregor, P. Rosa, R. S. Pulwarty, E. L. F. Schipper, B. T. Sinh, H. Décamps, et al. Determinants of risk: exposure and vulnerability. In *Managing the risks of extreme events and disasters to advance climate change adaptation: special report of the intergovernmental panel on climate change*, pages 65–108. Cambridge University Press, 2012.
- M. Çelik, Ö. Ergun, B. Johnson, P. Keskinocak, Á. Lorca, P. Pekgün, and J. Swann. Humanitarian logistics. In *New directions in informatics, optimization, logistics, and production*, pages 18–49. INFORMS, 2012.
- H.-S. Chang and C.-H. Liao. Planning emergency shelter locations based on evacuation behavior. *Natural Hazards*, 76(3):1551–1571, 2015.
- M.-S. Chang, Y.-L. Tseng, and J.-W. Chen. A scenario planning approach for the flood emergency logistics preparation problem under uncertainty. *Transportation Research Part E: Logistics and Transportation Review*, 43(6):737–754, 2007.
- S. Chanta and O. Sangsawang. Shelter-site selection during flood disaster. *Lecture Notes in Management Science*, 4: 282–288, 2012.

- Z. Chen, X. Chen, Q. Li, and J. Chen. The temporal hierarchy of shelters: A hierarchical location model for earthquake-shelter planning. *International Journal of Geographical Information Science*, 27(8):1612–1630, 2013.
- C. J. Chiappetta Jabbour, V. A. Sobreiro, A. B. Lopes de Sousa Jabbour, L. M. de Souza Campos, E. B. Mariano, and D. W. S. Renwick. An analysis of the literature on humanitarian logistics and supply chain management: Paving the way for future studies. *Annals of Operations Research*, 283:289–307, 2019.
- R. L. Church. Geographical information systems and location science. *Computers & Operations Research*, 29(6):541–562, 2002.
- S. Cohen, A. Raney, D. Munasinghe, J. D. Loftis, A. Molthan, J. Bell, L. Rogers, J. Galantowicz, G. R. Brakenridge, A. J. Kettner, et al. The floodwater depth estimation tool (FwDET v2.0) for improved remote sensing analysis of coastal flooding. *Natural Hazards and Earth System Sciences*, 19(9):2053–2065, 2019.
- J. Coutinho-Rodrigues, L. Tralhão, and L. Alçada-Almeida. Solving a location-routing problem with a multiobjective approach: The design of urban evacuation plans. *Journal of Transport Geography*, 22:206–218, 2012.
- T. J. Cova, P. E. Dennison, and F. A. Drews. Modeling evacuate versus shelter-in-place decisions in wildfires. *Sustainability*, 3(10):1662–1687, 2011.
- J. Dalal and H. Üster. Combining worst case and average case considerations in an integrated emergency response network design problem. *Transportation Science*, 52(1):171–188, 2018.
- H. De Vries and L. N. Van Wassenhove. Do optimization models for humanitarian operations need a paradigm shift? *Production and Operations Management*, 29(1):55–61, 2020.
- E. W. Dijkstra. A note on two problems in connexion with graphs. *Numerische Mathematik*, 1(1):269–271, 1959.
- K. F. Doerner, W. J. Gutjahr, and P. C. Nolz. Multi-criteria location planning for public facilities in tsunami-prone coastal areas. *OR Spectrum*, 31:651–678, 2009.
- Z. Dönmez, B. Y. Kara, Ö. Karsu, and F. Saldanha-da Gama. Humanitarian facility location under uncertainty: Critical review and future prospects. *Omega*, 102:102393, 2021.
- D. Eckstein, V. Künzel, L. Schäfer, and M. Wings. Global Climate Risk Index 2020. Bonn: Germanwatch, 2019. URL https://www.germanwatch.org/sites/germanwatch.org/files/20-2-01e%20Global%20Climate%20Risk%20Index%202020_13.pdf.
- J. R. Eiser, A. Bostrom, I. Burton, D. M. Johnston, J. McClure, D. Paton, J. Van Der Pligt, and M. P. White. Risk interpretation and action: A conceptual framework for responses to natural hazards. *International Journal of Disaster Risk Reduction*, 1:5–16, 2012.
- EM-DAT. Disasters Year in Review 2021. URL: <https://cred.be/downloadFile.php?file=sites/default/files/CredCrunch66.pdf>, 2021.
- S. Eom, M. Umamoto, and T. Suzuki. Cross-border evacuation and intermunicipal cooperation during large-scale flood disasters. *International Journal of Disaster Risk Reduction*, 79:103159, 2022.
- J. Ercolano. Pedestrian disaster preparedness and emergency management of mass evacuations on foot: State-of-the-art and best practices. *Journal of Applied Security Research*, 3(3-4):389–405, 2008.
- R. Z. Farahani, M. Lotfi, A. Baghaian, R. Ruiz, and S. Rezapour. Mass casualty management in disaster scene: A systematic review of OR&MS research in humanitarian operations. *European Journal of Operational Research*, 287(3):787–819, 2020.
- J.-E. Faucher, S. Dávila, and X. Hernández-Cruz. Modeling pedestrian evacuation for near-field tsunamis fusing ALCD and agent-based approaches: a case study of Rincón, PR. *International Journal of Disaster Risk Reduction*, 49:101606, 2020.
- FEMA. Risk MAP products. URL: <https://www.fema.gov/flood-maps/tools-resources/risk-map/products> (Accessed 2023-11-07), 2023.
- G. Galindo and R. Batta. Review of recent developments in OR/MS research in disaster operations management. *European Journal of Operational Research*, 230(2):201–211, 2013.
- M. Gama, B. F. Santos, and M. P. Scaparra. A multi-period shelter location-allocation model with evacuation orders for flood disasters. *EURO Journal on Computational Optimization*, 4(3-4):299–323, 2016.
- S. Gupta, N. Altay, and Z. Luo. Big data in humanitarian supply chain management: A review and further research directions. *Annals of Operations Research*, 283(1):1153–1173, 2019.
- W. J. Gutjahr and P. C. Nolz. Multicriteria optimization in humanitarian aid. *European Journal of Operational Research*, 252(2):351–366, 2016.
- J. Hallak, M. Koyuncu, and P. Miç. Determining shelter locations in conflict areas by multiobjective modeling: A case study in northern Syria. *International Journal of Disaster Risk Reduction*, 38:101202, 2019.
- K. Haynes, L. Coates, R. Leigh, J. Handmer, J. Whittaker, A. Gissing, J. McAneney, and S. Opper. ‘Shelter-in-place’vs. evacuation in flash floods. *Environmental Hazards*, 8(4):291–303, 2009.

- I. Heckmann, T. Comes, and S. Nickel. A critical review on supply chain risk—Definition, measure and modeling. *Omega*, 52:119–132, 2015.
- V. Heimhuber, J.-C. Hannemann, and W. Rieger. Flood risk management in remote and impoverished areas—a case study of onaville, haiti. *Water*, 7(7):3832–3860, 2015.
- M. C. Hoyos, R. S. Morales, and R. Akhavan-Tabatabaei. OR models with stochastic components in disaster operations management: A literature survey. *Computers & Industrial Engineering*, 82:183–197, 2015.
- INFORM. Index for Risk Management – Results 2016, 2016. URL <https://drmkc.jrc.ec.europa.eu/inform-index/Portals/0/InfoRM/Publications/INFORM%20Annual%20Report%202016.pdf>.
- N. Insani, D. Akman, S. Taheri, and J. Hearne. Short-notice flood evacuation plan under dynamic demand in high populated areas. *International Journal of Disaster Risk Reduction*, 74:102844, 2022.
- J. G. Jin, Y. Shen, H. Hu, Y. Fan, and M. Yu. Optimizing underground shelter location and mass pedestrian evacuation in urban community areas: A case study of Shanghai. *Transportation Research Part A: Policy and Practice*, 149:124–138, 2021.
- L. M. Johnston, X. Wang, S. Erni, S. W. Taylor, C. B. McFayden, J. A. Oliver, C. Stockdale, A. Christianson, Y. Boulanger, S. Gauthier, et al. Wildland fire risk research in Canada. *Environmental Reviews*, 28(2):164–186, 2020.
- B. Y. Kara and M.-È. Rancourt. Location problems in humanitarian supply chains. In G. Laporte, S. Nickel, and F. Saldanha da Gama, editors, *Location Science*, chapter 21, pages 611–629. Springer Nature Switzerland, second edition, 2019.
- B. Y. Kara and S. Savaşer. Humanitarian logistics. In *Leading developments from INFORMS communities*, pages 263–303. INFORMS, 2017.
- M. M. Kassem, F. M. Nazri, and E. N. Farsangi. Development of seismic vulnerability index methodology for reinforced concrete buildings based on nonlinear parametric analyses. *MethodsX*, 6:199–211, 2019.
- S. Khalilpourazari and S. H. R. Pasandideh. Designing emergency flood evacuation plans using robust optimization and artificial intelligence. *Journal of Combinatorial Optimization*, 41:640–677, 2021.
- F. Kilci, B. Y. Kara, and B. Bozkaya. Locating temporary shelter areas after an earthquake: A case for Turkey. *European Journal of Operational Research*, 243(1):323–332, 2015.
- Ö. B. Kınay, B. Y. Kara, F. Saldanha-da Gama, and I. Correia. Modeling the shelter site location problem using chance constraints: A case study for Istanbul. *European Journal of Operational Research*, 270(1):132–145, 2018.
- Ö. B. Kınay, F. Saldanha-da Gama, and B. Y. Kara. On multi-criteria chance-constrained capacitated single-source discrete facility location problems. *Omega*, 83:107–122, 2019.
- S. Kongsomsaksakul, C. Yang, and A. Chen. Shelter location-allocation model for flood evacuation planning. *Journal of the Eastern Asia Society for Transportation Studies*, 6:4237–4252, 2005.
- G. Kovacs and M. Moshtari. A roadmap for higher research quality in humanitarian operations: A methodological perspective. *European Journal of Operational Research*, 276(2):395–408, 2019.
- G. Kovacs, M. Moshtari, H. Kachali, and P. Polska. Research methods in humanitarian logistics. *Journal of Humanitarian Logistics and Supply Chain Management*, 9(3):325–331, 2019.
- W. Kron. Flood risk = Hazard . Values . Vulnerability. *Water International*, 30(1):58–68, 2005.
- N. Kunz, L. N. Van Wassenhove, M. Besiou, C. Hambye, and G. Kovacs. Relevance of humanitarian logistics research: best practices and way forward. *International Journal of Operations & Production Management*, 37(11):1585–1599, 2017.
- G. Laporte. Fifty years of operational research: 1972–2022. *European Journal of Operational Research*, 2023.
- H.-K. Lee, W.-H. Hong, and Y.-H. Lee. Experimental study on the influence of water depth on the evacuation speed of elderly people in flood conditions. *International Journal of Disaster Risk Reduction*, 39:101198, 2019.
- A. C. Li, L. Nozick, N. Xu, and R. Davidson. Shelter location and transportation planning under hurricane conditions. *Transportation Research Part E: Logistics and Transportation Review*, 48(4):715–729, 2012.
- L. Li, M. Jin, and L. Zhang. Sheltering network planning and management with a case in the Gulf Coast region. *International Journal of Production Economics*, 131(2):431–440, 2011.
- F. Liberatore, C. Pizarro, C. Blas, M. Ortuño, and B. Vitoriano. Uncertainty in humanitarian logistics for disaster management. A review. In *Decision aid models for disaster management and emergencies*, pages 45–74. Springer, 2013.
- H. R. Lim, M. Lim, B. Bernadeth, and M. Piantanakulchai. Determinants of household flood evacuation mode choice in a developing country. *Natural Hazards*, 84(1):507–532, 2016.
- J. Llopis Abella, E. B. Perge, Z. Afif, C. R. Soto Orozco, L. M. Padilla, and J. Hsu. Using behavioral insights to improve disaster preparedness, early warning and response mechanisms in Haiti, 2020.

- H. Lukosch and T. Comes. Gaming as a research method in humanitarian logistics. *Journal of Humanitarian Logistics and Supply Chain Management*, 9(3):352–370, 2019.
- A. Mansourian, A. Rajabifard, M. V. Zoej, and I. Williamson. Using SDI and web-based system to facilitate disaster management. *Computers & Geosciences*, 32(3):303–315, 2006.
- M. Marin-Ferrer, L. Vernaccini, and K. Poljansek. *INFORM Index for Risk Management – Concept and Methodology Version 2017*. European Union, 2017. doi: 10.2760/094023.
- J. McGlade, G. Bankoff, J. Abrahams, S. Cooper-Knock, F. Cotecchia, P. Desanker, W. Erian, E. Gencer, L. Gibson, S. Girgin, et al. Global assessment report on disaster risk reduction 2019, 2019.
- M. Merz, M. Hiete, T. Comes, and F. Schultmann. A composite indicator model to assess natural disaster risks in industry on a spatial level. *Journal of Risk Research*, 16(9):1077–1099, 2013.
- D. S. Mileti, J. H. Sorensen, and P. W. O’Brien. Toward an explanation of mass care shelter use in evacuations. *International Journal of Mass Emergencies and Disasters*, 10(1):25–42, 1992.
- C. Miller and A. A. Ager. A review of recent advances in risk analysis for wildfire management. *International Journal of Wildland Fire*, 22(1):1–14, 2012.
- H. Nakanishi, J. Black, and Y. Suenaga. Investigating the flood evacuation behaviour of older people: A case study of a rural town in Japan. *Research in Transportation Business & Management*, 30:100376, 2019.
- Z. Nedović-Budić and J. K. Pinto. Interorganizational GIS: Issues and prospects. *The Annals of Regional Science*, 33: 183–195, 1999.
- E. Ozbay, Ö. Çavuş, and B. Y. Kara. Shelter site location under multi-hazard scenarios. *Computers & Operations Research*, 106:102–118, 2019.
- M. Papathoma-Köhle, M. Schlögl, and S. Fuchs. Vulnerability indicators for natural hazards: An innovative selection and weighting approach. *Scientific Reports*, 9(1):15026, 2019.
- M. Papathoma-Köhle, M. Schlögl, C. Garlich, M. Diakakis, S. Mavroulis, and S. Fuchs. A wildfire vulnerability index for buildings. *Scientific Reports*, 12(1):6378, 2022.
- J. A. Paul and X. J. Wang. Robust location-allocation network design for earthquake preparedness. *Transportation Research Part B: Methodological*, 119:139–155, 2019.
- A. J. Pedraza-Martinez and L. N. Van Wassenhove. Empirically grounded research in humanitarian operations management: The way forward. *Journal of Operations Management*, 45(1):1–10, 2016.
- A. J. Pedraza-Martinez, O. Stapleton, and L. N. Van Wassenhove. On the use of evidence in humanitarian logistics research. *Disasters*, 37:S51–S67, 2013.
- F. Pérez-Galarce, L. J. Canales, C. Vergara, and A. Candia-Véjar. An optimization model for the location of disaster refuges. *Socio-Economic Planning Sciences*, 59:56–66, 2017.
- M.-È. Rancourt, J.-F. Cordeau, G. Laporte, and B. Watkins. Tactical network planning for food aid distribution in Kenya. *Computers & Operations Research*, 56:68–83, 2015.
- J. Rentschler, M. Salhab, and B. A. Jafino. Flood exposure and poverty in 188 countries. *Nature Communications*, 13 (1):3527, 2022.
- O. Rodríguez-Espíndola and J. Gaytán. Scenario-based preparedness plan for floods. *Natural Hazards*, 76(2):1241–1262, 2015.
- O. Rodríguez-Espíndola, P. Albores, and C. Brewster. GIS and optimisation: Potential benefits for emergency facility location in humanitarian logistics. *Geosciences*, 6(2):18, 2016.
- O. Rodríguez-Espíndola, P. Albores, and C. Brewster. Disaster preparedness in humanitarian logistics: A collaborative approach for resource management in floods. *European Journal of Operational Research*, 264(3):978–993, 2018.
- S. Rufat, E. Tate, C. G. Burton, and A. S. Maroof. Social vulnerability to floods: Review of case studies and implications for measurement. *International Journal of Disaster Risk Reduction*, 14:470–486, 2015.
- M. Sabbaghtorkan, R. Batta, and Q. He. Prepositioning of assets and supplies in disaster operations management: Review and research gap identification. *European Journal of Operational Research*, 284(1):1–19, 2020.
- F. S. Salman and E. Yücel. Emergency facility location under random network damage: Insights from the Istanbul case. *Computers & Operations Research*, 62:266–281, 2015.
- G. Saunders. Post-disaster shelter: Ten designs. IFRC: International Federation of Red Cross and Red Crescent Societies, 2013.
- J. Scanlon. Evacuations and Shelter. *Disaster Preparedness: Some Myths and Misconceptions*, 1992.
- J.-B. Sheu and C. Pan. A method for designing centralized emergency supply network to respond to large-scale natural disasters. *Transportation Research Part B: Methodological*, 67:284–305, 2014.
- K. Y. Sokat, I. S. Dolinskaya, K. Smilowitz, and R. Bank. Incomplete information imputation in limited data environments with application to disaster response. *European Journal of Operational Research*, 269(2):466–485, 2018.

- S. Song, H. Zhou, and W. Song. Sustainable shelter-site selection under uncertainty: A rough QUALIFLEX method. *Computers & Industrial Engineering*, 128:371–386, 2019.
- Sphere Association. Sphere handbook: Humanitarian charter and minimum standards in humanitarian response. URL: www.spherestandards.org/handbook, 2018.
- T. A. Steelman and S. McCaffrey. Best practices in risk and crisis communication: Implications for natural hazards management. *Natural Hazards*, 65(1):683–705, 2013.
- J. Teng, D. Penton, C. Ticehurst, A. Sengupta, A. Freebairn, S. Marvanek, J. Vaze, M. Gibbs, N. Streeton, F. Karim, et al. A comprehensive assessment of floodwater depth estimation models in semiarid regions. *Water Resources Research*, 58(11):e2022WR032031, 2022.
- M. P. Thompson, T. Zimmerman, D. Mindar, and M. A. Taber. *Risk terminology primer: Basic principles and a glossary for the wildland fire management community*. United States Department of Agriculture, Forest Service, Rocky Mountain, 2016.
- P. Tran, R. Shaw, G. Chantry, and J. Norton. GIS and local knowledge in disaster management: A case study of flood risk mapping in Viet Nam. *Disasters*, 33(1):152–169, 2009.
- A. Trivedi and A. Singh. A multi-objective approach for locating temporary shelters under damage uncertainty. *International Journal of Operational Research*, 38(1):31–48, 2020.
- B. L. Turner, R. E. Kasperson, P. A. Matson, J. J. McCarthy, R. W. Corell, L. Christensen, N. Eckley, J. X. Kasperson, A. Luers, M. L. Martello, et al. A framework for vulnerability analysis in sustainability science. *Proceedings of the National Academy of Sciences*, 100(14):8074–8079, 2003.
- United Nations. General Assembly - Report of the open-ended intergovernmental expert working group on indicators and terminology relating to disaster risk reduction, 2016. URL <https://undocs.org/en/A/71/644>.
- U.S. Army Corps of Engineers Hydrologic Engineering Center. HEC-RAS. URL: <https://www.hec.usace.army.mil/software/hec-ras/> (Accessed 2023-11-21), 2023.
- L. N. Van Wassenhove. Humanitarian aid logistics: supply chain management in high gear. *Journal of the Operational Research Society*, 57(5):475–489, 2006.
- L. White, H. Smith, and C. Currie. OR in developing countries: A review. *European Journal of Operational Research*, 208(1):1–11, 2011.
- N. Wood, J. Jones, M. Schmittlein, J. Schelling, and T. Frazier. Pedestrian flow-path modeling to support tsunami evacuation and disaster relief planning in the US Pacific Northwest. *International Journal of Disaster Risk Reduction*, 18:41–55, 2016.
- N. Wood, J. Jones, J. Peters, and K. Richards. Pedestrian evacuation modeling to reduce vehicle use for distant tsunami evacuations in Hawai'i. *International Journal of Disaster Risk Reduction*, 28:271–283, 2018.
- World Bank. Haiti - Strengthening Disaster Risk Management and Climate Resilience Project. URL: <https://documents.worldbank.org/en/publication/documents-reports/documentdetail/595131556810024755/haiti-strengthening-disaster-risk-management-and-climate-resilience-project>, 2019a.
- World Bank. Haiti - Flood Hazard Maps. URL: <https://datacatalog.worldbank.org/search/dataset/0048128/Haiti---Flood-Hazard-Maps>, 2019b.
- World Bank. The world bank in haiti. URL: <https://www.worldbank.org/en/country/haiti>, 2022.
- World Bank. Haiti - flood hazard maps. URL: <https://datacatalog.worldbank.org/search/dataset/0048128/Haiti---Flood-Hazard-Maps> (Accessed 2023-11-07), 2023.
- WRI. The number of people affected by floods will double between 2010 and 2030. URL: <https://www.wri.org/insights/number-people-affected-floods-will-double-between-2010-and-2030>, 2020.

A Computing the percentage of uncovered people in the existing network

In order to compute the percentage of uncovered people in the existing network, we need to determine how many people are covered with the set of existing shelters denoted by J' , $J' \cap J = \emptyset$. If there are no existing shelters ($J' = \emptyset$), then the percentage of uncovered people is 100%. Otherwise, we need to solve a mathematical model. In the following, we detail how to compute the percentage of uncovered people when $J' \neq \emptyset$.

When $J' \neq \emptyset$, we solve the following model to determine the percentage of uncovered people with the existing network:

$$\text{Model 3} \quad \min \quad \theta_1 \sum_{j \in J'} \sum_{i \in W_j(r)} -\tilde{r}_i^p p_i x_{ij} + \theta_2 \sum_{j \in J'} \tilde{r}_j^s q_j y_j + \theta_3 \sum_{j \in J'} \sum_{i \in W_j(r)} \tilde{r}_{ij}^e p_i x_{ij} \quad (6a)$$

$$\text{s.t.} \quad \sum_{i \in W_j(r)} p_i x_{ij} \leq q_j y_j, \quad j \in J' \quad (6b)$$

$$\sum_{j \in V_i(r) \cap J'} x_{ij} \leq 1, \quad i \in I \quad (6c)$$

$$x_{ij} \geq 0, \quad i \in I, j \in J' \quad (6d)$$

$$y_j \in \{0, 1\}, \quad j \in J'. \quad (6e)$$

This model is similar to Model 1 but has not budget constraints. In addition, for the set J' , the normalized population risk is measured by assuming that the percentage of uncovered people is 100%.

In our set of experiments, we restrict ourselves to the weights $\theta_1 = \theta_2 = \theta_3 = 0.33$ when solving Model 2. Using the optimal solution of Model 2, the number of covered people in the existing network is computed as $\tilde{p}_i = \sum_{j \in J'} \sum_{i \in W_j(r)} p_i \tilde{x}_{ij}^{(2)}$, where $\tilde{x}_{ij}^{(2)}$ represents the values of the x -variables in the optimal solution of Model 2. Then, for each population point, we compute the percentage of uncovered people in the existing network as $(1 - \tilde{p}_i/p_i)$.

B Normalization of the risk measures

In this section, we explain how the population risk, the shelter risk and the evacuation risk have been normalized. The data was normalized by using standard methods considering the interquartile range (IQR) and winsorizing for outlier values. Using the concept of IQR, and defining Q1 and Q3 as the first and third quartile, all values that are below Q1 - 1.5 IQR, and all values that are above Q3 + 1.5 IQR are considered as outliers, i.e., lower outliers and upper outliers. Winsorizing is then used by setting all values below Q1 - 1.5 IQR to Q1 - 1.5 IQR, and all values above Q3 + 1.5 IQR to Q3 + 1.5 IQR. Using the resulting data, it is then scaled to a $[0, 1]$ -range. In the following, we provide the detailed notation to explain how each risk measure has been normalized.

The normalized population risk, $\tilde{r}_i^p, i \in I$, is computed as follows. As previously explained, all values in $\tilde{r}_i^p, i \in I$ are winsorized using 1.5 IQR, and the resulting risk is denoted by \widehat{r}_i^p . Then, the normalized

value is obtained by dividing the resulting risk by its risk interval, that is,

$$\tilde{r}_i^p = \frac{\widehat{r}_i^p - \min_{i \in I} \widehat{r}_i^p}{\max_{i \in I} \widehat{r}_i^p - \min_{i \in I} \widehat{r}_i^p}, \forall i \in I. \quad (7)$$

The normalized shelter risk, $\tilde{r}_j^s, j \in J \cup J'$, is computed for 1) the normalized shelter risk for new potential shelters and 2) the normalized shelter risk for existing shelters. For the normalized shelter risk for new potential shelters, all values in $r_j^s, j \in J$ are winsorized using 1.5 IQR, and the resulting risk is denoted by \widehat{r}_j^s . Similarly, for the normalized shelter risk for existing shelters, all values in $r_j^s, j \in J'$ are winsorized using 1.5 IQR, and the resulting risk is denoted by \widehat{r}_j^s . Then, the normalized value is obtained by dividing the resulting risk by its risk interval, that is,

$$\tilde{r}_j^s = \frac{\widehat{r}_j^s - \min_{j \in J} \widehat{r}_j^s}{\max_{j \in J} \widehat{r}_j^s - \min_{j \in J} \widehat{r}_j^s}, \forall j \in J, \quad (8)$$

and

$$\tilde{r}_j^s = \frac{\widehat{r}_j^s - \min_{j \in J'} \widehat{r}_j^s}{\max_{j \in J'} \widehat{r}_j^s - \min_{j \in J'} \widehat{r}_j^s}, \forall j \in J'. \quad (9)$$

The normalized evacuation risk is computed for all pairs of population points i and shelters j within the maximal coverage radius r , that is, $\tilde{r}_{ij}^e, i \in I, j \in V_i(r)$. Similarly to the normalized shelter risk it is computed for 1) the evacuation towards new potential shelters and 2) the evacuation towards existing shelters. For the normalized evacuation risk towards new potential shelters, all values in $r_{ij}^e, i \in I, j \in V_i(r) \cap J$ are winsorized using 1.5 IQR, and the resulting risk is denoted by \widehat{r}_{ij}^e . Similarly, for the normalized evacuation risk towards existing shelters, all values in $r_{ij}^e, i \in I, j \in V_i(r) \cap J'$ are winsorized using 1.5 IQR, and the resulting risk is denoted by \widehat{r}_{ij}^e . Then, the normalized value is obtained by dividing the resulting risk by its risk interval, that is,

$$\tilde{r}_{ij}^e = \frac{\widehat{r}_{ij}^e - \min_{i \in I, j \in V_i(r) \cap J} \widehat{r}_{ij}^e}{\max_{i \in I, j \in V_i(r) \cap J} \widehat{r}_{ij}^e - \min_{i \in I, j \in V_i(r) \cap J} \widehat{r}_{ij}^e}, \forall i \in I, j \in V_i(r) \cap J, \quad (10)$$

and

$$\tilde{r}_{ij}^e = \frac{\widehat{r}_{ij}^e - \min_{i \in I, j \in V_i(r) \cap J'} \widehat{r}_{ij}^e}{\max_{i \in I, j \in V_i(r) \cap J'} \widehat{r}_{ij}^e - \min_{i \in I, j \in V_i(r) \cap J'} \widehat{r}_{ij}^e}, \forall i \in I, j \in V_i(r) \cap J'. \quad (11)$$

C Building the *road layer*

In the following, we first describe the data extracted from OpenStreetMap. Then, we explain how this data was connected with our shelter network (population points and shelters) to create the *road layer*.

First, from OpenStreetMap, we extracted a network $\mathcal{G} = (\mathcal{N}, \mathcal{A})$, where \mathcal{N} represents a set of single points in space (referred to as the set of nodes) and \mathcal{A} represents the set of road segments (referred

to as the set of arcs). Each node $n \in \mathcal{N}$ is associated with a latitude and a longitude. Each arc $(k, n) \in \mathcal{A}$ is associated with a source node $k \in \mathcal{N}$, a destination node $n \in \mathcal{N}$, and a distance \tilde{d}_{kn} (in km). In the case of pedestrian-based evacuation, we assume that a road can be used in any direction. Therefore, if there exists two arcs between the same pair of nodes, that is $(k, n), (n, k) \in \mathcal{A}, k, n \in \mathcal{N}$, then we set the distance of arcs (k, n) and (n, k) as $(\tilde{d}_{kn} + \tilde{d}_{nk})/2$.

Second, we had to connect the *OSM data* with our set of population points I and shelters $J \cup J'$. Therefore, using the *population layer*, *existing shelter layer*, *potential new shelter layer*, and *OSM layer*, we created an additional layer referred to as the *road layer*. This *road layer* is represented by the network $\mathbf{G} = (\mathbf{N}', \mathbf{A}')$. The set of increased nodes comprises the original set of nodes \mathcal{N} as well as all the population and shelter vertices, that is, $\mathbf{N}' = \mathcal{N} \cup I \cup J \cup J'$. Because vertices V are not in the *OSM layer*, they had to be connected to the road network. Therefore, the set of increased arcs is defined as $\mathbf{A}' = \mathcal{A} \cup \{(i, n) : i \in I, n \in \mathcal{N}, d_{in} \leq r_1\} \cup \{(n, j) : n \in \mathcal{N}, j \in J \cup J', d_{nj} \leq r_2\}$ as the original set of arcs as well as arcs between the population points and nodes within a radius r_1 , and arcs between nodes and shelters within a radius r_2 . Note that the distances $d_{in}, i \in I, n \in \mathcal{N}$ and $d_{nj}, n \in \mathcal{N}, j \in J \cup J'$ are computed as an Euclidean distance. In addition, after discussions with the H-SDRMCRP team, the values of r_1 and r_2 were set to 3 and 0.25 km.

D Determining the travel time from $i \in I$ to $j \in J \cup J'$

In this section, we explain how the travel time from $i \in I$ to $j \in J \cup J'$ has been estimated. First, we provide an estimate for the evacuation travel time of each arc in \mathbf{A}' . Second, because multiple paths can exist from $i \in I$ to $j \in J \cup J'$, a Dijkstra shortest-path algorithm is used to compute the shortest path (using the evacuation travel time) between each population point $i \in I$ and shelter $j \in J \cup J'$.

First, to determine the travel time of each arc \mathbf{A}' , we have to determine the evacuation speed which represents the walking speed according to the flood depth. Note that the evacuation speed is measured in kilometer per hour (km/h). Using the ‘‘Mean’’ values from Table 3 in [Bernardini et al. \(2020\)](#) (by converting the flood depth in meters and the walking speed in km/h), we conducted a linear regression to determine the evacuation speed. Figure 9 presents the converted ‘‘Mean’’ values from Table 3 (the speed in km/h according to the flood depth in meters) with our linear regression. This linear regression led us to compute the evacuation speed of each node of the increased network, i.e., $n \in \mathbf{N}'$, as

$$\phi_k = \max\{0, -1.2446f_k^d + 3.3861\} \quad (12)$$

where f_k^d is flood depth of node k in meters. For population points ($i \in I$), this value is set as f_i^d as defined in Section 5.2. For shelters ($j \in J \cup J'$), this value is set as f_j^d as defined in Section 5.3. For all other nodes ($n \in \mathcal{N}$), we defined a square buffer of 5m x 5m around each node $n \in \mathcal{N}$ and conducted ‘‘zonal statistics’’ by overlapping the *flood layer* with the *road layer*. We then obtained for each buffer around a node its average flood depth which was defined as $f_n^d, n \in \mathcal{N}$. For each arc $(n, k) \in \mathbf{A}'$, if $\phi_n + \phi_k > 0$, its evacuation travel time is then computed as

$$\frac{\tilde{d}_{nk}}{(\phi_n + \phi_k)/2}, \quad (13)$$

otherwise, if $\phi_n + \phi_k = 0$, then its evacuation time is 0.

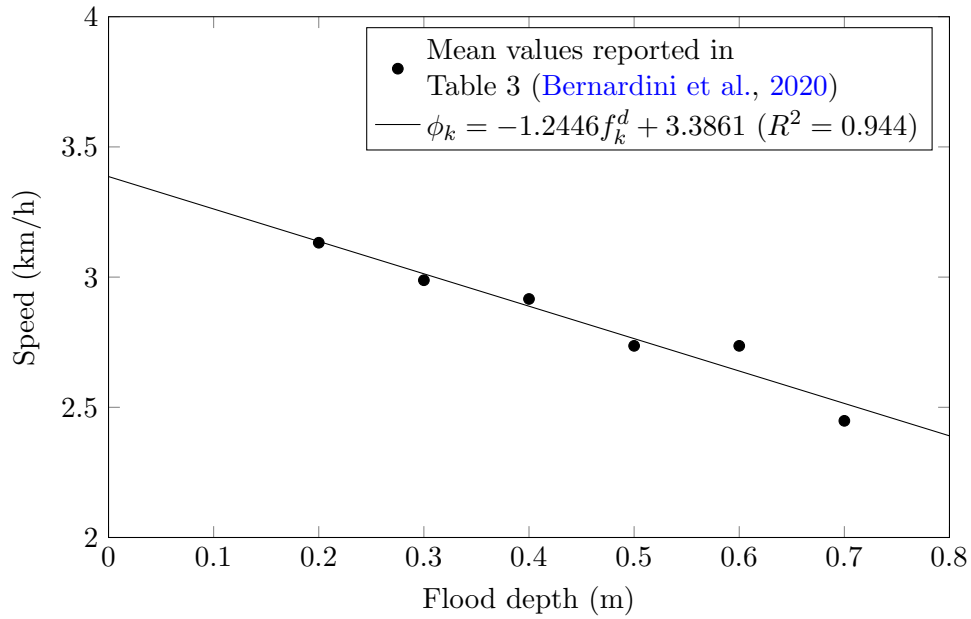


Fig. 9: Linear regression with the mean values reported in Table 3 of Bernardini et al. (2020)

Second, in graph $\mathbf{G} = (\mathbf{N}', \mathbf{A}')$, there might exist multiple paths between a given population point $i \in I$ and a given shelter $j \in J \cup J'$. Therefore, a Dijkstra shortest-path algorithm (Dijkstra, 1959) is used to determine the shortest evacuation travel time (as computed in Equation 13) from each population point $i \in I$ to each shelter location j . This shortest evacuation travel time corresponds to $t_{ij}, (i, j) \in E$.